

**Analytical framework for the substitution of steel-concrete composite columns with equivalent steel columns in structural design**

PAPAVASILEIOU, Georgios

Available from Sheffield Hallam University Research Archive (SHURA) at:

<http://shura.shu.ac.uk/32229/>

---

This document is the author deposited version. You are advised to consult the publisher's version if you wish to cite from it.

**Published version**

PAPAVASILEIOU, Georgios (2017). Analytical framework for the substitution of steel-concrete composite columns with equivalent steel columns in structural design. *ESR Journal*, 2 (1).

---

**Copyright and re-use policy**

See <http://shura.shu.ac.uk/information.html>

## RESEARCH ARTICLE

# Analytical framework for the substitution of steel-concrete composite columns with equivalent steel sections in structural design


Georgios S. Papavasileiou\*

Department of Mechanical Engineering, University of Applied Sciences of Thessaly, Larissa, Greece

\*Corresponding author: Georgios S. Papavasileiou  
email: george.papav@gmail.com, gpapav@teilar.gr

## Abstract:

The present work presents a mathematical framework to simulate steel-concrete composite columns with equivalent steel columns. A total number of three simulation methods are presented, in order to simulate circular and rectangular concrete-filled hollow sections, as well as concrete-encased I-shaped sections with steel columns of similar shape. The simulation is achieved by the satisfaction of three equations regarding their (a) axial resistance, (b) flexural stiffness about the major axis and (c) flexural stiffness about the minor axis. Solution of the aforementioned provides the dimensions of the equivalent steel sections as functions of the characteristics of the steel-concrete composite sections (a) in a closed form for all hollow sections and (b) in a high-accuracy approximate solution for I-shaped sections. The accuracy of the proposed methods and their general applicability are evaluated. The results yielded are indicative of the effectiveness of the proposed methods.

 Open Access Article

**Citation:** G. S. Papavasileiou (2017)  
Analytical framework for the substitution of steel-concrete composite columns with equivalent steel sections in structural design. ESR Journal 2(1)

**Received:** 11<sup>th</sup> September 2016

**Accepted:** 10<sup>th</sup> February 2017

**Published:** 13<sup>th</sup> February 2017

**Copyright:** © 2017 This is an open access article under the terms of the [Creative Commons Attribution License](#), which permits unrestricted use, distribution, and reproduction in any medium, provided the original author and source are credited.

**Funding:** The author received no specific funding for this work.

**Competing Interests:** The author has declared that no competing interests exist.

**Keywords:** steel-concrete composite, steel sections, columns, equivalence

## Introduction

Steel-concrete composite elements were initially used as a means to increase the fire-resistance of steel elements. However, they have proven to be particularly cost-effective as they use a relatively low-cost material, *i.e.* concrete, in order to substitute a proportion of the required steel. There are numerous applications of composite structures, especially in tall buildings. In civil engineering practice, though, steel-concrete composite elements are not often used in conventional building, mainly due to the lack of suitable finite element software.

Literature on the performance of steel-concrete composite columns is particularly rich, while new original research articles on the topic seem to be published in an increasing rate. The topic first investigated was the performance of concrete-filled circular hollow sections (CFCHS) (1-15). There is also abundance of investigations on concrete-filled rectangular hollow sections (CFRHS), such as (16-28), as well as experimental works comparing the performance of CFRHS and CFCHS, such as (29-32). The majority of the

available literature on their behavior dates back to the 1980s (33-45), while such elements have been constructed since the end of the 19th century.

However, despite the wealth of scientific knowledge available on composite columns, the existing engineering software focuses mainly on the design of pure-steel or reinforced concrete elements. Hence, in order to render their design possible using any structural engineering software, composite sections could be simulated using equivalent pure-steel sections. In conventional buildings, the elements mainly designed as steel-concrete composite are the columns and slabs, while use of composite beams is particularly limited. In the work of Papavasileiou (46), an extensive investigation on the simulation of composite columns was performed, in order to define a mathematical framework which would provide solutions in closed form, or of particularly high accuracy. A similar work, dealing only with partially-encased I-shaped sections was performed by Marinopoulou *et al.* (47). In both works it is pointed out that the internal stresses developed in columns subjected to gravitational or seismic loads, are mainly axial force and bi-axial bending, while shear forces are particularly low compared to their capacity. Hence, in order to simulate a column's performance, an equivalent fictitious section should have the same axial resistance and flexural stiffness about the major and minor axes. Furthermore, in order to allow the application of the proposed methods for the determination of alternatives in practice, the geometry of the fictitious sections should not differ substantially from that of the composite steel-concrete sections (e.g. simulating a concrete-encased I-shaped section with a circular one).

## Simulation of concrete-filled circular sections

Two equations need to apply for the simulation of steel-concrete composite double-symmetrical circular column sections with pure steel sections: (a) of their axial resistance and (b) of their flexural stiffness. The computational advantage of concrete-filled circular sections over concrete-filled rectangular sections is that their flexural stiffness is the same in all directions. However, when reinforcing steel is installed for safety reasons when designing against fire-induced damage scenarios, the stiffness of circular sections depends on the direction of lateral loading considered. In this work, the number of installed longitudinal reinforcement is considered to be a product of 4 (*i.e.*  $N_{\text{bars}} = 4n$ , where  $n$  is an integer), so that the stiffness of the section about  $y$ -axis is the same as its stiffness about  $z$ -axis. The geometrical characteristics of the steel-concrete composite and the fictitious pure-steel section are illustrated in Fig. 1.

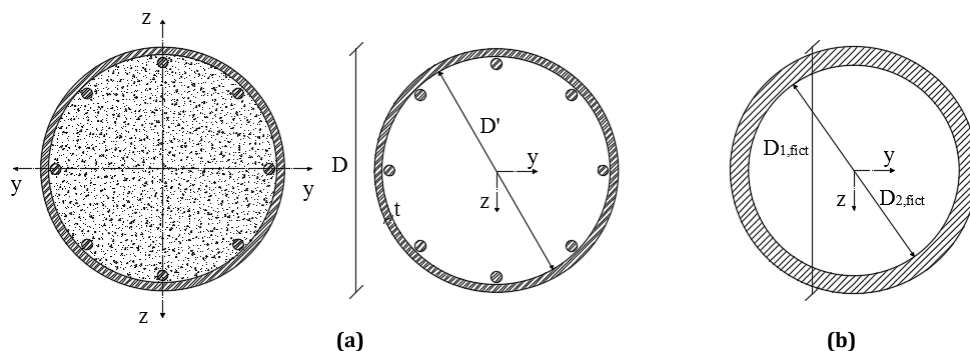


**Figure 1.** Geometric characteristics of the (a) composite concrete-filled and (b) fictitious pure-steel circular hollow section.

Since all bars have the same diameter, the total area of the reinforcement is a product of the area of a single bar multiplied by the number of bars (Eqn. 2.1).

$$A_{s,tot} = N_{bars} \cdot \left( \frac{\pi \cdot d^2}{4} \right) = 4 \cdot n \cdot \left( \frac{\pi \cdot d^2}{4} \right) = n \cdot \pi \cdot d^2 \quad (2.1)$$

The flexural stiffness provided by each bar to the composite section is the summation of the flexural stiffness of the bar and the additional stiffness calculated by the parallel axis theorem. The axis around which the stiffness is calculated is herein referred to as “reference axis”. For any value of n selected, there will be two bars the central axis of which is exactly on the reference axis, as well as two bars with a distance equal to the radial distance (*i.e.* the maximum distance). All other bars will have a distance of  $R_{S,i}$ . The value of  $R_{S,i}$  depends on the value of n, while at any case there will be 4 bars with the same distance from the reference axis. The flexural stiffness of an individual bar is calculated as:

$$I_{s,bar} = \left( \frac{\pi \cdot r^4}{4} \right) = \left( \frac{\pi \cdot \left( \frac{d}{2} \right)^4}{4} \right) \Rightarrow I_{s,bar} = \left( \frac{\pi \cdot d^4}{64} \right) \quad (2.2)$$

The additional stiffness due to the parallel axis theorem is:

$$I_{s,bar}^{add} = \left( \frac{\pi \cdot d^2}{4} \right) \cdot R_{S,i}^2 \Rightarrow I_{s,bar}^{add} = \left( \frac{\pi \cdot d^2}{4} \right) \cdot \left( \frac{d^2}{16} + R_{S,i}^2 \right) \quad (2.3)$$

Hence, the total flexural stiffness of the reinforcement is calculated as the summation of the flexural stiffness of all bars (Eqns. 2.2 and 2.3). Introducing the normalized variable  $r_{s,i} = R_{s,i}/d$ , the total stiffness of the reinforcement is provided in Eqn. 2.4.

$$\begin{aligned} I_s &= N \cdot \left( \frac{\pi \cdot d^4}{64} \right) + \left( \frac{\pi \cdot d^2}{4} \right) \cdot \sum_{i=1}^N R_{S,i}^2 \Rightarrow I_s = \left( \frac{\pi \cdot d^2}{4} \right) \cdot \left( N \cdot \frac{d^2}{16} + R_S^2 \cdot \sum_{i=1}^{4n} r_{S,i}^2 \right) \Rightarrow \\ I_s &= \left( \frac{\pi \cdot d^2}{4} \right) \cdot \left[ 4 \cdot n \cdot \frac{d^2}{16} + R_S^2 \cdot \left( 2 + 0 + 4 \cdot \sum_{i=1}^{\frac{4n-4}{4}} r_{S,i}^2 \right) \right] \Rightarrow \\ I_s &= \left( \frac{\pi \cdot d^2}{4} \right) \cdot \left[ n \cdot \frac{d^2}{4} + 2 \cdot R_S^2 \cdot \left( 1 + 2 \cdot \sum_{i=1}^{n-1} r_{S,i}^2 \right) \right] \end{aligned} \quad (2.4)$$

The axial resistance and flexural stiffness of the steel circular hollow section are calculated in Eqns. 2.5 and 2.6 respectively.

$$\begin{aligned} A_a &= \left( \frac{\pi \cdot D^2}{4} \right) - \left( \frac{\pi \cdot (D-2 \cdot t)^2}{4} \right) = \frac{\pi}{4} \cdot (D^2 - (D-2 \cdot t)^2) \Rightarrow \\ A_a &= \frac{\pi}{4} \cdot (D - (D-2 \cdot t)) \cdot (D + (D-2 \cdot t)) = \frac{\pi}{4} \cdot (2 \cdot t) \cdot (2 \cdot D - 2 \cdot t) \Rightarrow \\ A_a &= \pi \cdot t \cdot (D - t) \end{aligned} \quad (2.5)$$

$$\begin{aligned} I_a &= \left( \frac{\pi \cdot D^4}{64} \right) - \left( \frac{\pi \cdot (D-2 \cdot t)^4}{64} \right) = \frac{\pi}{64} \cdot (D^4 - (D-2 \cdot t)^4) \Rightarrow \\ I_a &= \frac{\pi}{64} \cdot (D^2 - (D-2 \cdot t)^2) \cdot (D^2 + (D-2 \cdot t)^2) \Rightarrow \\ I_a &= \frac{\pi}{8} \cdot t \cdot (D - t) \cdot (D \cdot (D - t) + 2 \cdot t^2) \end{aligned} \quad (2.6)$$

The total area and flexural stiffness of the concrete section (Eqns. 2.7 and 2.8 respectively) can be calculated considering a solid circular section from which

the corresponding characteristics of the longitudinal reinforcement provided in Eqns. 2.1 and 2.4, are subtracted.

$$A_c = \left( \frac{\pi \cdot D^2}{4} \right) - A_a - A_s = \left( \frac{\pi \cdot D^2}{4} \right) - \pi \cdot t \cdot (D-t) - n \cdot \left( \frac{\pi \cdot d^2}{4} \right) \Rightarrow$$

$$A_c = \left( \frac{\pi}{4} \right) \cdot (D^2 - 4 \cdot D \cdot t + 4 \cdot t^2) - n \cdot \left( \frac{\pi \cdot d^2}{4} \right) = \left( \frac{\pi \cdot (D-2 \cdot t)^2}{4} \right) - n \cdot \left( \frac{\pi \cdot d^2}{4} \right) \Rightarrow$$

$$A_c = \left( \frac{\pi}{4} \right) \cdot \left( (D-2 \cdot t)^2 - n \cdot d^2 \right) \quad (2.7)$$

$$I_c = \left( \frac{\pi \cdot D^4}{64} \right) - I_a - I_s \Rightarrow I_c = \left( \frac{\pi \cdot D^4}{64} \right) - \frac{\pi}{8} \cdot t \cdot (D-t) \cdot (D \cdot (D-t) + 2 \cdot t^2) - I_s \Rightarrow$$

$$I_c = \left( \frac{\pi \cdot (D-2 \cdot t)^4}{64} \right) - \left( \frac{\pi \cdot d^2}{4} \right) \cdot \left[ n \cdot \frac{d^2}{4} + 2 \cdot R_s^2 \cdot \left( 1 + 2 \cdot \sum_{i=1}^{n-1} r_{s,i}^2 \right) \right] \quad (2.8)$$

The fictitious pure-steel section is a circular hollow section made out of steel of the same grade as that of the composite section. The variables required for its definition are the external and internal diameter. The thickness of the section is simply calculated as half their difference:  $t_{fict} = (D_{1,fict} - D_{2,fict})/2$ . Eqns. 2.9 and 2.10 provide the formulas for the calculation of the total area and second moment of area of the fictitious section.

$$A_{fict} = \left( \frac{\pi}{4} \right) \cdot (D_{1,fict}^2 - D_{2,fict}^2) \quad (2.9)$$

$$I_{fict} = \frac{\pi}{64} \cdot (D_{1,fict}^4 - D_{2,fict}^4) \quad (2.10)$$

The ratio of the internal diameter over the external one is defined as  $\beta$ , so  $D_{2,fict} = \beta \cdot D_{1,fict}$ . Since  $D_{1,fict} > D_{2,fict}$ ,  $\beta \in (0; 1]$ . Also, the ratio of  $D_{1,fict}$  over  $D$  is defined as  $\alpha$ . So, the two variables used herein are  $\alpha$  and  $\beta$ . Additionally, in order to normalize the yielding/cracking stress of the materials, the variables  $\varphi_c$  and  $\varphi_s$  are introduced. Their values are determined by dividing the cracking stress of concrete and the yielding stress of reinforcing steel by the yielding stress of structural steel:  $\phi_c = f_c/f_a$  and  $\phi_s = f_s/f_a$ . Also, the area of the structural steel is normalized dividing by the total area of the composite section:  $A_a/A_{tot} = \rho_a$  and the area of reinforcing steel is normalized dividing by the area of the concrete:  $\rho_s = A_s/A_c \Rightarrow A_s = \rho_s \cdot A_c$ . Finally, the variables  $\rho'_a = 1 - \rho_a$  and  $\rho'_s = 1 + \rho_s$  are introduced in order to simplify the final equations. Using the aforementioned, the area of the concrete is calculated as:

$$A_a + A_c + A_s = \frac{\pi \cdot D^2}{4} \Rightarrow A_a + A_c + \rho_s \cdot A_c = \frac{\pi \cdot D^2}{4} \Rightarrow$$

$$A_a + (1 + \rho_s) \cdot A_c = \frac{\pi \cdot D^2}{4} \Rightarrow \rho_a \cdot \left( \frac{\pi \cdot D^2}{4} \right) + (1 + \rho_s) \cdot A_c = \frac{\pi \cdot D^2}{4} \Rightarrow$$

$$(1 + \rho_s) \cdot A_c = (1 - \rho_a) \cdot \left( \frac{\pi \cdot D^2}{4} \right) \Rightarrow A_c = \frac{(1 - \rho_a)}{(1 + \rho_s)} \cdot \left( \frac{\pi \cdot D^2}{4} \right) = \frac{\rho'_a}{\rho'_s} \cdot \left( \frac{\pi \cdot D^2}{4} \right) \quad (2.11)$$

Using the equilibrium of the axial resistance for the steel-concrete composite section (48) and the fictitious pure-steel section (49), a relationship between the two variables is defined. The final expression of the equation is defined by substituting the section areas using Eqns. 2.1, 2.5, 2.9 and 2.11 and normalizing by the total area of the composite section (*i.e.*  $A_{s,l} = \pi D^2/4$ ).

$$\begin{aligned}
 N_{Rd}^{fict} = N_{Rd}^{act} &\Rightarrow A_{fict} \cdot f_a = A_a \cdot f_a + A_c \cdot f_c + A_s \cdot f_s \Rightarrow \\
 \frac{\pi \cdot (D_{1,fict}^2 - D_{2,fict}^2)}{4} \cdot f_a &= A_a \cdot f_a + A_c \cdot f_c + A_s \cdot f_s \Rightarrow \\
 (1 - \beta^2) \cdot \left( \frac{\pi \cdot D_{1,fict}^2}{4} \right) \cdot f_a &= A_a \cdot f_a + A_c \cdot f_c + A_s \cdot f_s \Rightarrow \\
 \frac{(1 - \beta^2) \cdot \left( \frac{\pi \cdot D_{1,fict}^2}{4} \right) \cdot f_a}{f_a} &= \frac{A_a \cdot f_a}{f_a} + \frac{A_c \cdot f_c}{f_a} + \frac{A_s \cdot f_s}{f_a} \Rightarrow \\
 (1 - \beta^2) \cdot \left( \frac{\pi \cdot D_{1,fict}^2}{4} \right) &= A_a + A_c \cdot \phi_c + A_s \cdot \phi_s \Rightarrow \\
 \frac{(1 - \beta^2) \cdot \left( \frac{\pi \cdot D_{1,fict}^2}{4} \right)}{\left( \frac{\pi \cdot D^2}{4} \right)} &= \frac{A_a + A_c \cdot \phi_c + A_s \cdot \phi_s}{\left( \frac{\pi \cdot D^2}{4} \right)} \Rightarrow \\
 a^2 \cdot (1 - \beta^2) &= \rho_a + \left( \frac{4 \cdot A_c}{\pi \cdot D^2} \right) \cdot (\phi_c + \rho_s \cdot \phi_s) \Rightarrow \\
 a^2 \cdot (1 - \beta^2) &= \rho_a + \frac{\rho'_a}{\rho'_s} \cdot (\phi_c + \rho_s \cdot \phi_s) \tag{2.12}
 \end{aligned}$$

A second relationship between  $D_{1,fict}$  and  $\beta$  is defined by the equilibrium of the flexural stiffness of the actual and the fictitious sections. In order to normalize the flexural stiffness of the concrete and the reinforcing steel, the ratio of the Young's modulus of each material over that of the structural steel is introduced:  $\psi_c = E_c / E_a$  and  $\psi_s = E_s / E_a$ . The remaining dimensions are normalized as:  $d/D = \delta$ ,  $R_s/D = r_s$  and  $t/D = \vartheta$ .

$$\begin{aligned}
 E_a \cdot I_{fict} = (E \cdot I)_{tot,act} &\Rightarrow E_a \cdot I_{fict} = E_a \cdot I_a + E_c \cdot I_c + E_s \cdot I_s \Rightarrow \\
 \frac{E_a \cdot I_{fict}}{E_a \cdot \left( \frac{\pi \cdot D^4}{64} \right)} &= \frac{E_a \cdot I_a}{E_a \cdot \left( \frac{\pi \cdot D^4}{64} \right)} + \frac{E_c \cdot I_c}{E_a \cdot \left( \frac{\pi \cdot D^4}{64} \right)} + \frac{E_s \cdot I_s}{E_a \cdot \left( \frac{\pi \cdot D^4}{64} \right)} \Rightarrow \\
 \frac{(D_{1,fict}^4 - D_{2,fict}^4)}{D^4} &= \frac{8 \cdot t \cdot (D - t) \cdot (D(D - t) + 2 \cdot t^2)}{D^4} + \psi_c \cdot \frac{64 \cdot I_c}{\pi \cdot D^4} + \psi_s \cdot \frac{64 \cdot I_s}{\pi \cdot D^4} \Rightarrow \\
 \frac{(D_{1,fict}^4 - D_{2,fict}^4)}{D^4} &= 8 \cdot \theta \cdot (1 - \theta) \cdot ((1 - \theta) + 2 \cdot \theta^2) + \psi_c \cdot \frac{(D - 2 \cdot t)^4}{D^4} + (\psi_s - \psi_c) \cdot \frac{64 \cdot I_s}{\pi \cdot D^4} \Rightarrow \\
 \alpha^4 \cdot (1 - \beta^4) &= 8 \cdot \theta \cdot (1 - \theta) \cdot ((1 - \theta) + 2 \cdot \theta^2) + \psi_c \cdot (1 - 2 \cdot \theta)^4 + (\psi_s - \psi_c) \cdot \frac{64 \cdot I_s}{\pi \cdot D^4} \Rightarrow \\
 \alpha^4 (1 - \beta^4) &= 8\theta(1 - \theta)((1 - \theta) + 2\theta^2) + \psi_c(1 - 2\theta)^4 + N\delta^4 + 32\delta^2 r_s^2 \left( 1 + 2 \sum_{i=1}^{n-1} r_{s,i}^2 \right) \tag{2.13}
 \end{aligned}$$

Since the expressions on the right side of the Eqns. 2.12 and 2.13 are the summation of products of positive numbers, they are apparently positive numbers. Hence, in order to simplify the solution of the set of equations, they are replaced by the positive variables  $d_x^2$  and  $d_y^2$  respectively. So, Eqns. 2.12 and 2.13 are transformed to Eqns. 2.14 and 2.15 respectively.

$$a^2 \cdot (1 - \beta^2) = d_x^2 \tag{2.14}$$

$$a^4 \cdot (1 - \beta^4) = (a^2 \cdot (1 - \beta^2)) \cdot (a^2 \cdot (1 + \beta^2)) = d_y^2 \tag{2.15}$$

Dividing Eqns. 2.14 and 2.15 and solving for  $\alpha^2$ , its value is defined as a function of  $\beta^2$ .

$$\frac{(a^2 \cdot (1 - \beta^2)) \cdot (a^2 \cdot (1 + \beta^2))}{a^2 \cdot (1 - \beta^2)} = \frac{d_y^2}{d_x^2} \Rightarrow a^2 \cdot (1 + \beta^2) = d_y^2 / d_x^2 \Rightarrow a^2 = \frac{(d_y^2 / d_x^2)}{(1 + \beta^2)} \quad (2.16)$$

Substituting  $\alpha^2$  in Eqn. 2.14, using Eqn. 2.16 and solving for  $\beta$ , its value is determined in Eqn. 2.17.

$$\frac{(d_y^2 / d_x^2)}{(1 + \beta^2)} \cdot (1 - \beta^2) = d_x^2 \Rightarrow (1 - \beta^2) = \left( \frac{(d_x^2)^2}{d_y^2} \right) \cdot (1 + \beta^2) \Rightarrow 2 \cdot \beta^2 = 1 - \left( \frac{(d_x^2)^2}{d_y^2} \right) \Rightarrow$$

$$\beta = \sqrt{\frac{1 - ((d_x^2)^2 / d_y^2)}{2}} \quad (2.17)$$

Hence, substituting  $\beta$  in Eqn. 2.16 and solving for  $\alpha$ , its value is defined in Eqn. 2.18:

$$a^2 = \frac{d_x^2}{\left( 1 - \frac{1 - ((d_x^2)^2 / d_y^2)}{2} \right)} = \left( \frac{2 \cdot d_x^2}{1 + ((d_x^2)^2 / d_y^2)} \right) \Rightarrow a = \sqrt{\frac{2 \cdot d_x^2}{1 + ((d_x^2)^2 / d_y^2)}} \quad (2.18)$$

### Simulation of concrete-filled rectangular sections

In order to simulate the performance of concrete-filled rectangular sections, a procedure similar to that performed for circular sections is selected. However, since the flexural stiffness of rectangular sections about y-axis (major axis) is increased compared to that about z-axis (minor axis), two equilibriums of stiffness need to apply (one for each direction), as well as the equilibrium of axial resistance. The additional equilibrium is necessary because, in order to define a fictitious rectangular hollow section, three variables need to be determined: the height, the breadth and the thickness of the section. Fig. 2 illustrates the geometrical characteristics of the steel-concrete composite section. It should be noted that, in this Section, longitudinal reinforcement is also taken into consideration, as it could be used for fire-resistance purposes, even though its use in practice is not compulsory.

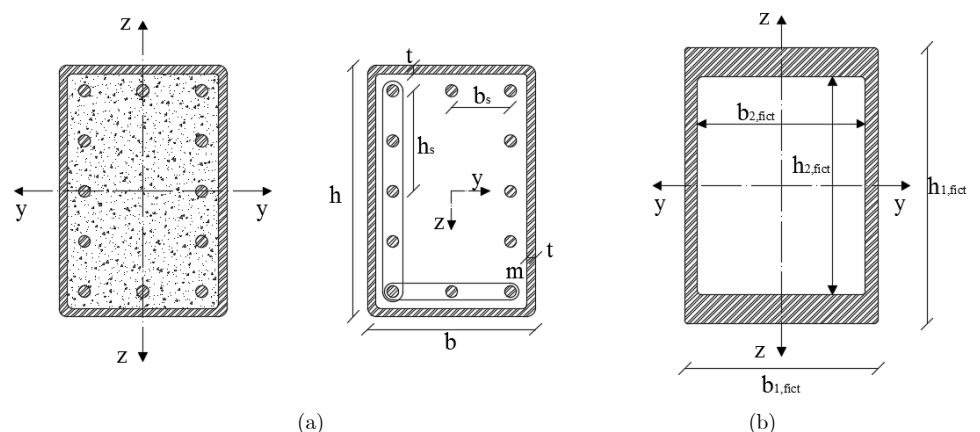


Figure 2. Geometric characteristics of the (a) composite concrete-filled and (b) fictitious pure-steel rectangular hollow section.

The total area of the longitudinal reinforcement (Eqn. 3.1) is simply calculated as the area of a single bar multiplied by the number of bars installed. In sections with a rectangular shape the same number of bars would be installed

in both directions. However, the larger the ratio of height over breadth is, the more bars would be required on the large sides of the column in order to confine concrete during a fire-induced damaged scenario.

$$A_{s,tot} = (2 \cdot n + 2 \cdot m - 4) \cdot A_s = (2 \cdot n + 2 \cdot m - 4) \cdot \left( \frac{\pi \cdot d^2}{4} \right) \quad (3.1)$$

The second moment of area of the longitudinal reinforcement is calculated as the second moment of area of a single bar multiplied by the number of bars used and the summation of the additional second moment of area for each bar calculated using the parallel axis theorem. Since the bars' section is circular, their second moment of area is the same about both axes, so the first part (Eqn. 3.2) is the same for both axes. For both axes there are bars which have the maximum distance from the reference axis (*i.e.*  $h_s$  for the calculation of  $I_y$  and  $b_s$  for the calculation of  $I_z$ ), bars with intermediate distance from it (*i.e.*  $h_{s,i}$  for y-axis and  $b_{s,i}$  for z-axis) and bars directly on the reference axis. Those bars provide the values  $I_{y,1}^{add}$  (Eqn. 3.3),  $I_{y,2}^{add}$  (Eqn. 3.4), 0 for y-axis and  $I_{z,1}^{add}$  (Eqn. 3.6),  $I_{z,2}^{add}$  (Eqn. 3.7), 0 for z-axis respectively. Hence, the total second moment of area for the longitudinal reinforcement is calculated in Eqn. 3.5 about the major axis and Eqn. 3.8 about the minor axis.

$$I_{R,tot} = (2 \cdot n + 2 \cdot m - 4) \cdot I_{R,\rho\acute{\alpha}\beta\delta\sigma\nu} = (2 \cdot n + 2 \cdot m - 4) \cdot \left( \frac{\pi \cdot d^4}{64} \right) \quad (3.2)$$

$$I_{y,1}^{add} = 2 \cdot m \cdot A_s \cdot h_s^2 = 2 \cdot m \cdot \left( \frac{\pi \cdot d^2}{4} \right) \cdot h_s^2 \quad (3.3)$$

$$I_{y,2}^{add} = 2 \cdot \left( \frac{\pi \cdot d^2}{4} \right) \cdot \sum_{i=1}^{n-2} h_{s,i}^2 \quad (3.4)$$

$$I_{y,s} = I_{R,tot} + I_{y,1}^{plus} + I_{y,2}^{plus} \Rightarrow$$

$$I_{y,s} = (2 \cdot n + 2 \cdot m - 4) \cdot \left( \frac{\pi \cdot d^4}{64} \right) + 2 \cdot m \cdot \left( \frac{\pi \cdot d^2}{4} \right) \cdot h_s^2 + 2 \cdot \left( \frac{\pi \cdot d^2}{4} \right) \cdot \sum_{i=1}^{n-2} h_{s,i}^2 \Rightarrow$$

$$I_{y,s} = 2 \cdot \left( \frac{\pi \cdot d^2}{4} \right) \cdot \left[ (n + m - 2) \cdot \left( \frac{d^2}{16} \right) + m \cdot h_s^2 + \sum_{i=1}^{n-2} h_{s,i}^2 \right] \quad (3.5)$$

$$I_{z,1}^{plus} = 2 \cdot n \cdot I_{z,\rho\acute{\alpha}\beta\delta\sigma\nu}^{plus} = 2 \cdot n \cdot \left( \frac{\pi \cdot d^2}{4} \right) \cdot b_s^2 \quad (3.6)$$

$$I_{z,2}^{plus} = 2 \cdot \left( \frac{\pi \cdot d^2}{4} \right) \cdot \sum_{i=1}^{m-2} b_{s,i}^2 \quad (3.7)$$

$$I_{z,s} = I_{R,tot} + I_{z,1}^{plus} + I_{z,2}^{plus} \Rightarrow$$

$$I_{z,s} = (2 \cdot n + 2 \cdot m - 4) \cdot \left( \frac{\pi \cdot d^4}{64} \right) + 2 \cdot n \cdot \left( \frac{\pi \cdot d^2}{4} \right) \cdot b_s^2 + 2 \cdot \left( \frac{\pi \cdot d^2}{4} \right) \cdot \sum_{i=1}^{m-2} b_{s,i}^2 \Rightarrow$$

$$I_{z,s} = 2 \cdot \left( \frac{\pi \cdot d^2}{4} \right) \cdot \left[ (n + m - 2) \cdot \left( \frac{d^2}{16} \right) + n \cdot b_s^2 + \sum_{i=1}^{m-2} b_{s,i}^2 \right] \quad (3.8)$$

Regarding the rectangular hollow section, the total area (Eqn. 3.9) and second moment of area about both axes (Eqns. 3.10 and 3.11) are calculate easily by subtracting the values corresponding to the internal rectangle, by those corresponding to the external one, as they have the same centroids.

$$A_a = b \cdot h - (b - 2 \cdot t) \cdot (h - 2 \cdot t) = b \cdot h - b \cdot h + 2 \cdot b \cdot t + 2 \cdot h \cdot t - 4 \cdot t^2 \Rightarrow$$



$$A_a = 2t \cdot (b + h - 2 \cdot t) \quad (3.9)$$

$$I_{y,a} = \left( \frac{b \cdot h^3}{12} \right) - \left( \frac{(b-2 \cdot t) \cdot (h-2 \cdot t)^3}{12} \right) \Rightarrow I_{y,a} = \left( \frac{b \cdot h^3}{12} \right) - (1-2 \cdot \theta_b) \cdot (1-2 \cdot \theta_h)^3 \cdot \left( \frac{b \cdot h^3}{12} \right) \Rightarrow$$

$$I_{y,a} = (1 - (1-2 \cdot \theta_b) \cdot (1-2 \cdot \theta_h)^3) \cdot \left( \frac{b \cdot h^3}{12} \right) \quad (3.10)$$

$$I_{z,a} = \left( \frac{b^3 \cdot h}{12} \right) - \left( \frac{(b-2 \cdot t)^3 \cdot (h-2 \cdot t)}{12} \right) \Rightarrow I_{z,a} = \left( \frac{b^3 \cdot h}{12} \right) - (1-2 \cdot \theta_b)^3 \cdot (1-2 \cdot \theta_h) \cdot \left( \frac{b^3 \cdot h}{12} \right) \Rightarrow$$

$$I_{z,a} = (1 - (1-2 \cdot \theta_b)^3 \cdot (1-2 \cdot \theta_h)) \cdot \left( \frac{b^3 \cdot h}{12} \right) \quad (3.11)$$

Due to the existence of longitudinal reinforcement, the section of the concrete is irregular. However, since its centroids overlap those of the steel section and the reinforcement, its area (Eqn. 3.12) and second moment of area (Eqns. 3.13 and 3.14) are calculated by subtracting the values corresponding to the aforementioned from those of the solid rectangular section defined by its height and breadth. In order to express the equations as a function of  $b$  and  $h$ , the ratios  $\theta_b = t/b$  and  $\theta_h = t/h$ . Their purpose is to allow for the quantities  $b \cdot h^3/12$  and  $h \cdot b^3/12$  to be extracted and, consequently, simplify the equations.

$$A_c = b \cdot h - A_a - A_s = b \cdot h - 2t \cdot (b + h - 2 \cdot t) - (2 \cdot n + 2 \cdot m - 4) \cdot \left( \frac{\pi \cdot d^2}{4} \right) \Rightarrow$$

$$A_c = b \cdot h - 2 \cdot t \cdot b - 2 \cdot t \cdot h + 4 \cdot t^2 - (2 \cdot n + 2 \cdot m - 4) \cdot \left( \frac{\pi \cdot d^2}{4} \right) \Rightarrow$$

$$A_c = (b - 2 \cdot t) \cdot (h - 2 \cdot t) - (2 \cdot n + 2 \cdot m - 4) \cdot \left( \frac{\pi \cdot d^2}{4} \right) \quad (3.12)$$

$$I_{y,c} = \left( \frac{b \cdot h^3}{12} \right) - I_{y,a} - I_{y,s} = \left( \frac{b \cdot h^3}{12} \right) - (1 - (1-2 \cdot \theta_b) \cdot (1-2 \cdot \theta_h)^3) \cdot \left( \frac{b \cdot h^3}{12} \right) - I_{y,s} \Rightarrow$$

$$I_{y,c} = (1 - 2 \cdot \theta_b) \cdot (1 - 2 \cdot \theta_h)^3 \cdot \left( \frac{b \cdot h^3}{12} \right) - I_{y,s} \Rightarrow$$

$$I_{y,c} = (1 - 2 \cdot \theta_b) \cdot (1 - 2 \cdot \theta_h)^3 \cdot \left( \frac{b \cdot h^3}{12} \right) - \left( \frac{\pi \cdot d^2}{2} \right) \cdot \left[ (n + m - 2) \cdot \left( \frac{d^2}{16} \right) + m \cdot h_s^2 + \sum_{i=1}^{n-2} h_{s,i}^2 \right] \quad (3.13)$$

$$I_{z,c} = \left( \frac{b^3 \cdot h}{12} \right) - I_{z,a} - I_{z,s} = \left( \frac{b^3 \cdot h}{12} \right) - (1 - (1-2 \cdot \theta_b)^3 \cdot (1-2 \cdot \theta_h)) \cdot \left( \frac{b^3 \cdot h}{12} \right) - I_{z,s} \Rightarrow$$

$$I_{z,c} = (1 - 2 \cdot \theta_b)^3 \cdot (1 - 2 \cdot \theta_h) \cdot \left( \frac{b^3 \cdot h}{12} \right) - I_{z,s} \Rightarrow$$

$$I_{z,c} = (1 - 2 \cdot \theta_b)^3 \cdot (1 - 2 \cdot \theta_h) \cdot \left( \frac{b^3 \cdot h}{12} \right) - \left( \frac{\pi \cdot d^2}{2} \right) \cdot \left[ (n + m - 2) \cdot \left( \frac{d^2}{16} \right) + n \cdot b_s^2 + \sum_{i=1}^{m-2} b_{s,i}^2 \right] \quad (3.14)$$

The definition of a fictitious pure-steel section with a uniform thickness was thoroughly investigated. However, approximations were required, so the resulting formulas yielded were not in closed form. The advantage of a closed form formula is that there is no deviation between the values obtained for the actual composite section and the fictitious pure-steel one. In order to allow for the definition of such formulas, the constraint on the thickness should be removed, so that the flexural stiffness about one axis can be increased without particular effect. However, as the number of variables increased to four, an additional equilibrium is required. This equilibrium was strategically selected in order to correlate the

variables to each other. Specifically, the ratio of the external dimensions should be equal to the ratio of the internal dimensions (Eqn. 3.15). Fig. 2.b illustrates the fictitious pure-steel rectangular hollow section. The thickness on each side can be calculated using the formulas provided in Eqns. 3.16 and 3.17.

$$\frac{b_{1,fict}}{h_{1,fict}} = \frac{b_{2,fict}}{h_{2,fict}} = \gamma \Rightarrow b_{1,fict} = \gamma \cdot b_{2,fict} \quad \text{and} \quad h_{1,fict} = \gamma \cdot h_{2,fict} \quad (3.15)$$

$$t_{H,fict} = \frac{h_{1,fict} - h_{2,fict}}{2} \quad (3.16)$$

$$t_{V,fict} = \frac{b_{1,fict} - b_{2,fict}}{2} \quad (3.17)$$

The total area and second moment of area of the fictitious section are calculated using the formulas that apply on the rectangular hollow section of the composite column. Introducing the variable  $\gamma$  (Eqn. 3.15), all formulas are expressed in Eqns. 3.18, 3.19 and 3.20 as a function of  $h_{1,fict}$ ,  $b_{1,fict}$  and  $\gamma$ .

$$A_{fict} = b_{1,fict} \cdot h_{1,fict} - b_{2,fict} \cdot h_{2,fict} = b_{1,fict} \cdot h_{1,fict} - \gamma \cdot b_{1,fict} \cdot \gamma \cdot h_{1,fict} \Rightarrow A_{fict} = (1 - \gamma^2) \cdot b_{1,fict} \cdot h_{1,fict} \quad (3.18)$$

$$I_{y,fict} = \frac{b_{1,fict} \cdot h_{1,fict}^3}{12} - \frac{b_{2,fict} \cdot h_{2,fict}^3}{12} = \frac{b_{1,fict} \cdot h_{1,fict}^3}{12} - \frac{\gamma \cdot b_{1,fict} \cdot \gamma^3 \cdot h_{1,fict}^3}{12} \Rightarrow I_{y,fict} = (1 - \gamma^4) \cdot \frac{b_{1,fict} \cdot h_{1,fict}^3}{12} \quad (3.19)$$

$$I_{z,fict} = \frac{b_{1,fict}^3 \cdot h_{1,fict}}{12} - \frac{b_{2,fict}^3 \cdot h_{2,fict}}{12} = \frac{b_{1,fict}^3 \cdot h_{1,fict}}{12} - \frac{\gamma^3 \cdot b_{1,fict}^3 \cdot \gamma \cdot h_{1,fict}}{12} \Rightarrow I_{z,fict} = (1 - \gamma^4) \cdot \frac{b_{1,fict}^3 \cdot h_{1,fict}}{12} \quad (3.20)$$

The definition of the unknown variables is achieved by the solution of the set of equations corresponding to the aforementioned equilibriums. The first equation is formulated by the equilibrium of axial resistances, substituting the respective areas from Eqns. 3.1, 3.9, 3.12 and 3.18.

$$N_{Rd}^{act} = N_{Rd}^{fict} \Rightarrow A_a \cdot f_a + A_c \cdot f_c + A_s \cdot f_s = A_{fict} \cdot f_a \Rightarrow A_a \cdot f_a + A_c \cdot f_c + A_s \cdot f_s = (1 - \gamma^2) \cdot b_{1,fict} \cdot h_{1,fict} \cdot f_a \quad (3.21)$$

Both sides of Eqn. 3.21 are divided by  $f_a$  and the variables  $\phi_c = f_c / f_a$ ,  $\rho_a = A_a / A_{tot}$  and  $\rho_a' = 1 - \rho_a$  are introduced in order to normalize the yielding/cracking stresses.

$$\frac{(1 - \gamma^2) \cdot b_{1,fict} \cdot h_{1,fict} \cdot f_a}{f_a} = \frac{A_a \cdot f_a}{f_a} + \frac{A_c \cdot f_c}{f_a} + \frac{A_s \cdot f_s}{f_a} \Rightarrow (1 - \gamma^2) \cdot b_{1,fict} \cdot h_{1,fict} = A_a + A_c \cdot \phi_c + A_s \cdot \phi_s \quad (3.22)$$

The area of the longitudinal bars ( $A_s$ ) can be replaced by a function of  $A_c$ , introducing their ratio  $\rho_s = A_s / A_c$ . From Eqn. 3.12, substituting the area of the structural steel and concrete, using the aforementioned, the area of concrete can be expressed as a function of  $b$  and  $h$  (Eqn. 3.23).

$$A_a + A_c + A_s = b \cdot h \Rightarrow A_a + A_c + \rho_s \cdot A_c = b \cdot h \Rightarrow A_a + (1 + \rho_s) \cdot A_c = b \cdot h \Rightarrow \rho_a \cdot b \cdot h + (1 + \rho_s) \cdot A_c = b \cdot h \Rightarrow (1 + \rho_s) \cdot A_c = (1 - \rho_a) \cdot b \cdot h \Rightarrow A_c = \frac{(1 - \rho_a)}{(1 + \rho_s)} \cdot b \cdot h = \frac{\rho_a'}{\rho_s'} \cdot b \cdot h \quad (3.23)$$

Finally, both sides of Eqn. 3.22 are divided by  $b \cdot h$  and the variables  $\beta = b_{1,fict} / b$  and  $\eta = h_{1,fict} / h$  are introduced. Hence, the first equilibrium, as well as the next two are herein expressed as functions of  $\beta$ ,  $\eta$  and  $\gamma$ .

$$\begin{aligned} \frac{(1-\gamma^2) \cdot b_{1,fict} \cdot h_{1,fict}}{b \cdot h} &= \frac{A_a}{b \cdot h} + \frac{A_c \cdot \phi_c}{b \cdot h} + \frac{A_s \cdot \phi_s}{b \cdot h} \Rightarrow \\ \frac{(1-\gamma^2) \cdot \beta \cdot b \cdot \eta \cdot h}{b \cdot h} &= \rho_\alpha + \frac{A_c \cdot \phi_c}{b \cdot h} + \frac{\rho_s \cdot A_c \cdot \phi_s}{b \cdot h} \Rightarrow \\ (1-\gamma^2) \cdot \beta \cdot \eta &= \rho_\alpha + (\phi_c + \rho_s \cdot \phi_s) \cdot \frac{\rho'_a}{\rho'_s} \end{aligned} \quad (3.24)$$

The second equation required for the definition of the fictitious section's geometrical characteristics derives from the equilibrium of flexural stiffness about the major axis (Eqn. 3.25). Substituting from Eqns. 3.5, 3.10, 3.13 and 3.19, the equilibrium of the stiffness about the major axis becomes:

$$(E \cdot I)_{y,act} = E_a \cdot I_{y,fict} \Rightarrow E_a \cdot I_{y,a} + E_c \cdot I_{y,c} + E_s \cdot I_{y,s} = E_a \cdot I_{y,fict} \quad (3.25)$$

Both sides of the equation are divided by  $E_a$  and the normalized variables  $\psi_c = E_c / E_a$  and  $\psi_s = E_s / E_a$  are introduced. Additional normalized values (Eqns. 3.26, 3.27, 3.28 and 3.29) are defined in order to allow for the simplification of the following formulas. In particular:

The diameter of the longitudinal reinforcement is normalized using:

$$\frac{d}{b} = \delta_b \quad \text{and} \quad \frac{d}{h} = \delta_h \quad (3.26)$$

The dimensions  $h_{s,i}$  and  $b_{s,i}$  are normalized using:

$$\frac{b_{s,i}}{b} = \beta_{s,i} \quad \text{and} \quad \frac{h_{s,i}}{h} = \eta_{s,i} \quad (3.27)$$

The thickness of the rectangular hollow section is normalized using:

$$\frac{t}{b} = \theta_b \quad \text{and} \quad \frac{t}{h} = \theta_h \quad (3.28)$$

The second moment of area provided by the reinforcement is normalized using:

$$\alpha_{s,y} = \frac{I_{y,s}}{(b \cdot h^3 / 12)} \quad (3.29)$$

Substituting  $I_{y,s}$  from Eqn. 3.5, and introducing the necessary normalized variables, the expression of  $\alpha_{s,y}$  is transformed as provided in Eqn. 3.30.

$$\begin{aligned} \alpha_{s,y} &= \frac{I_{y,s}}{b \cdot h^3} = \frac{2 \cdot \left( \frac{\pi \cdot d^2}{4} \right) \cdot \left[ (n+m-2) \cdot \left( \frac{d^2}{16} \right) + n \cdot h_s^2 + \sum_{i=1}^{n-2} h_{s,i}^2 \right]}{12 \cdot \frac{b \cdot h^3}{12}} \Rightarrow \\ \alpha_{s,y} &= 6 \cdot (\pi \cdot \delta_b \cdot \delta_h) \cdot \left[ (n+m-2) \cdot \left( \frac{\delta_h^2}{16} \right) + n \cdot \eta_s^2 + \sum_{i=1}^{n-2} \eta_{s,i}^2 \right] \end{aligned} \quad (3.30)$$

The normalized values  $\beta = b_{1,fict} / b$  and  $\eta = h_{1,fict} / h$  are introduced, in order to allow the resulting expression to be independent of the measurement units used. Substituting in Eqn. 3.25 the respective second moment of area expressions from Eqns. 3.5, 3.10, 3.13 and 3.19, dividing both sides of the equation by  $E_a \cdot b \cdot h^3 / 12$  and introducing the normalized variables described above, the equation forms as:

$$E_a \cdot I_{y,fict} = (E \cdot I)_{y,act} \Rightarrow E_a \cdot I_{y,fict} = E_a \cdot I_{y,a} + E_c \cdot I_{y,c} + E_s \cdot I_{y,s} \Rightarrow$$

$$\frac{E_a \cdot (1-\gamma^4) \cdot \frac{b_{1,fiat} \cdot h_{1,fiat}^3}{12}}{E_a \cdot \left(\frac{b \cdot h^3}{12}\right)} = \frac{E_a \cdot (1-(1-2\cdot\theta_b) \cdot (1-2\cdot\theta_h)^3) \cdot \left(\frac{b \cdot h^3}{12}\right) + E_c \cdot I_{y,c} + E_s \cdot I_{y,s}}{E_a \cdot \left(\frac{b \cdot h^3}{12}\right)} \Rightarrow$$

$$(1-\gamma^4) \cdot \beta \cdot \eta^3 = (1-(1-2\cdot\theta_b) \cdot (1-2\cdot\theta_h)^3) + \psi_c \cdot \frac{I_{y,c}}{\left(\frac{b \cdot h^3}{12}\right)} + \psi_s \cdot \frac{I_{y,s}}{\left(\frac{b \cdot h^3}{12}\right)} \Rightarrow$$

$$(1-\gamma^4) \cdot \beta \cdot \eta^3 = (1-(1-\psi_c) \cdot (1-2\cdot\theta_b) \cdot (1-2\cdot\theta_h)^3) + (\psi_s - \psi_c) \cdot a_{s,y} \quad (3.31)$$

Applying a similar procedure on the equilibrium of flexural stiffness about the minor axis, the third equation is formulated. The variable  $\alpha_{s,z}$  is designated as the ratio of  $I_{z,s}$  over  $b^3h/12$ , in order to simplify the expression of final equation. Using the expression of  $I_{z,s}$  defined in Eqn. 3.8 and using all aforementioned normalized values, the expression of  $\alpha_{s,z}$  is given in Eqn. 3.32.

$$\alpha_{s,z} = \frac{I_{z,s}}{\frac{b^3 \cdot h}{12}} = \frac{2 \cdot \left(\frac{\pi \cdot d^2}{4}\right) \cdot \left[(n+m-2) \cdot \left(\frac{d^2}{16}\right) + n \cdot b_s^2 + \sum_{i=1}^{m-2} b_{s,i}^2\right]}{\frac{b^3 \cdot h}{12}} \Rightarrow$$

$$\alpha_{s,z} = 6 \cdot (\pi \cdot \delta_b \cdot \delta_h) \cdot \left[(n+m-2) \cdot \left(\frac{\delta_b^2}{16}\right) + n \cdot \beta_s^2 + \sum_{i=1}^{m-2} \beta_{s,i}^2\right] \quad (3.32)$$

The second moment of area values of each constituting component are replaced by the formulas defined in Eqns. 3.8, 3.11, 3.14 and 3.20. Both sides of the equation are divided by  $E_a \cdot b^3h/12$ , and the equation is simplified to Eqn. 3.33.

$$E_a \cdot I_{z,fiat} = (E \cdot I)_{z,act} = E_a \cdot I_{z,a} + E_c \cdot I_{z,c} + E_s \cdot I_{z,s} \Rightarrow$$

$$\frac{E_a \cdot I_{z,fiat}}{E_a \cdot \frac{b^3 \cdot h}{12}} = \frac{E_a \cdot I_{z,a}}{E_a \cdot \frac{b^3 \cdot h}{12}} + \frac{E_c \cdot I_{z,c}}{E_a \cdot \frac{b^3 \cdot h}{12}} + \frac{E_s \cdot I_{z,s}}{E_a \cdot \frac{b^3 \cdot h}{12}} \Rightarrow$$

$$\frac{(1-\gamma^4) \cdot \frac{b_{1,fiat}^3 \cdot h_{1,fiat}}{12}}{\frac{b^3 \cdot h}{12}} = \frac{(1-(1-2\cdot\theta_b) \cdot (1-2\cdot\theta_h)^3) \cdot \left(\frac{b \cdot h^3}{12}\right)}{\frac{b^3 \cdot h}{12}} + \psi_c \cdot \frac{I_{z,c}}{\frac{b^3 \cdot h}{12}} + \psi_s \cdot \frac{I_{z,s}}{\frac{b^3 \cdot h}{12}} \Rightarrow$$

$$(1-\gamma^4) \cdot \beta^3 \cdot \eta = (1-(1-\psi_c) \cdot (1-2\cdot\theta_b) \cdot (1-2\cdot\theta_h)^3) + (\psi_s - \psi_c) \cdot a_{s,z} \quad (3.33)$$

The three equations forming the set under investigation are Eqns. 3.24, 3.31 and 3.33. In all the aforementioned, the expressions on the right side of the equation consist of variables with known values. By definition, the variables used on the left side are positive numbers, so their product is a positive number as well. Hence, the expressions on the right side are positive numbers, the value of which is known. Hence, in order to simplify the solution process, they are replaced by the positive variables  $d_x^2$ ,  $d_y^2$  and  $d_z^2$ , so Eqns. 3.24, 3.31 and 3.33 transform to Eqns. 3.34, 3.35 and 3.36.

$$(1-\gamma^2) \cdot \beta \cdot \eta = d_x^2 \quad (3.34)$$

$$(1-\gamma^4) \cdot \beta \cdot \eta^3 = d_y^2 \quad (3.35)$$

$$(1-\gamma^4) \cdot \beta^3 \cdot \eta = d_z^2 \quad (3.36)$$

Apparently,  $(1-\gamma^4) = [1^2 - (\gamma^2)^2] = (1-\gamma^2) \cdot (1+\gamma^2)$ . So, replacing it in Eqns. 3.35 and 3.36 and dividing by Eqn. 3.34, formulas giving  $\eta^2$  and  $\beta^2$  as functions of  $\gamma$  are received.

$$(1-\gamma^4) \cdot \beta \cdot \eta^3 = d_y^2 \Rightarrow (1-\gamma^2) \cdot (1+\gamma^2) \cdot \beta \cdot \eta \cdot \eta^2 = d_y^2 \Rightarrow$$

$$[(1-\gamma^2) \cdot \beta \cdot \eta] \cdot (1+\gamma^2) \cdot \eta^2 = d_y^2 \Rightarrow (1+\gamma^2) \cdot \eta^2 = \frac{d_y^2}{d_x^2} \Rightarrow \eta^2 = \frac{d_y^2/d_x^2}{(1+\gamma^2)} \quad (3.37)$$

$$(1-\gamma^4) \cdot \beta^3 \cdot \eta = d_z^2 \Rightarrow (1-\gamma^2) \cdot (1+\gamma^2) \cdot \beta \cdot \eta \cdot \beta^2 = d_z^2 \Rightarrow$$

$$[(1-\gamma^2) \cdot \beta \cdot \eta] \cdot (1+\gamma^2) \cdot \beta^2 = d_z^2 \Rightarrow (1+\gamma^2) \cdot \beta^2 = \frac{d_z^2}{d_x^2} \Rightarrow \beta^2 = \frac{d_z^2/d_x^2}{(1+\gamma^2)} \quad (3.38)$$

Multiplying Eqns. 3.37 and 3.38 and receiving their square root, an expression of  $\beta \cdot \eta$  as a function of  $\gamma$  is determined.

$$\beta^2 \cdot \eta^2 = \frac{d_y^2/d_x^2}{(1+\gamma^2)} \cdot \frac{d_z^2/d_x^2}{(1+\gamma^2)} \Rightarrow (\beta \cdot \eta)^2 = \frac{d_y^2 \cdot d_z^2 / (d_x^2)^2}{(1+\gamma^2)^2} \Rightarrow \beta \cdot \eta = \frac{\sqrt{d_y^2 \cdot d_z^2}}{d_x^2 \cdot (1+\gamma^2)} \quad (3.39)$$

Substituting the expression of  $\beta \cdot \eta$  from Eqn. 3.39 in Eqn. 3.34 and introducing the variable  $K = (d_z^2)^2 / \sqrt{d_z^2 \cdot d_y^2}$ , the equation can be solved for  $\gamma$ .

$$\frac{\sqrt{d_z^2 \cdot d_y^2}}{(d_z^2) \cdot (1+\gamma^2)} \cdot (1-\gamma^2) = d_x^2 \Rightarrow \frac{(1-\gamma^2)}{(1+\gamma^2)} = \frac{(d_z^2)^2}{\sqrt{d_z^2 \cdot d_y^2}} \Rightarrow \frac{(1-\gamma^2)}{(1+\gamma^2)} = K \Rightarrow$$

$$(1-\gamma^2) = (1+\gamma^2) \cdot K \Rightarrow 1-\gamma^2 = K + K \cdot \gamma^2 \Rightarrow$$

$$(1+K) \cdot \gamma^2 = (1-K) \Rightarrow \gamma^2 = \frac{(1-K)}{(1+K)} \Rightarrow \gamma = \sqrt{\frac{(1-K)}{(1+K)}} \Rightarrow$$

$$\gamma = \frac{\sqrt{\left(1 - \frac{(d_z^2)^2}{\sqrt{d_z^2 \cdot d_y^2}}\right)}}{\sqrt{\left(1 + \frac{(d_z^2)^2}{\sqrt{d_z^2 \cdot d_y^2}}\right)}} \Rightarrow \gamma = \frac{\sqrt{\sqrt{d_z^2 \cdot d_y^2} - (d_z^2)^2}}{\sqrt{\sqrt{d_z^2 \cdot d_y^2} + (d_z^2)^2}} \Rightarrow \gamma = \sqrt{1 - \frac{2 \cdot (d_z^2)^2}{\sqrt{d_z^2 \cdot d_y^2} + (d_z^2)^2}} \quad (3.40)$$

Variables  $\beta$  (Eqn. 3.41) and  $\eta$  (Eqn. 3.42) are determined by substituting the expression of  $\gamma$  in Eqns. 3.37 and 3.38 from Eqn. 3.40.

$$\eta^2 = \frac{d_y^2/d_x^2}{(1+\gamma^2)} \Rightarrow \eta = \sqrt{\frac{d_y^2/d_x^2}{(1+\gamma^2)}} \Rightarrow \eta = \frac{\sqrt{d_y^2/d_x^2}}{\sqrt{\left(1 + \left(\frac{\sqrt{\sqrt{d_z^2 \cdot d_y^2} - (d_z^2)^2}}{\sqrt{\sqrt{d_z^2 \cdot d_y^2} + (d_z^2)^2}}\right)^2\right)}} \Rightarrow$$

$$\eta = \frac{\sqrt{d_y^2/d_x^2}}{\sqrt{\left(1 + 1 - \frac{2 \cdot (d_z^2)^2}{\sqrt{d_z^2 \cdot d_y^2} + (d_z^2)^2}\right)}} \Rightarrow \eta = \frac{\sqrt{d_y^2/d_x^2}}{\sqrt{\left(\frac{2 \cdot \sqrt{d_z^2 \cdot d_y^2} + 2 \cdot (d_z^2)^2 - 2 \cdot (d_z^2)^2}{\sqrt{d_z^2 \cdot d_y^2} + (d_z^2)^2}\right)}} \Rightarrow$$

$$\eta = \sqrt{\frac{\left(\sqrt{\sqrt{d_z^2 \cdot d_y^2} + (d_z^2)^2}\right) \cdot d_y^2}{\left(2 \cdot \sqrt{d_z^2 \cdot d_y^2}\right) \cdot d_x^2}} \quad (3.41)$$

$$\beta^2 = \frac{d_z^2/d_x^2}{(1+\gamma^2)} \Rightarrow \beta = \sqrt{\frac{d_z^2/d_x^2}{(1+\gamma^2)}} \Rightarrow \beta = \frac{\sqrt{d_z^2/d_x^2}}{\sqrt{\left(1 + 1 - \frac{(d_z^2)^2}{\sqrt{d_z^2 \cdot d_y^2} + (d_z^2)^2}\right)}} \Rightarrow$$

$$\beta = \sqrt{\frac{\frac{d_z^2/d_x^2}{2 \cdot \sqrt{d_z^2 \cdot d_y^2 + 2 \cdot (d_z^2)^2 - (d_z^2)^2}}}{\sqrt{d_z^2 \cdot d_y^2 + (d_z^2)^2}}} \Rightarrow \beta = \sqrt{\frac{(\sqrt{d_z^2 \cdot d_y^2 + (d_z^2)^2}) \cdot d_z^2}{(2 \cdot \sqrt{d_z^2 \cdot d_y^2}) \cdot d_x^2}} \quad (3.42)$$

## Simulation of concrete-encased I-shaped sections

### Formulation of the mathematical simulation model

Concrete-encased steel I-shaped sections require the use of transversal reinforcement (stirrups) which, along with the longitudinal reinforcement confine the concrete core. Hence, the composite section resembles that of reinforced concrete one. However, particular provisions are required in order to ensure the composite performance of the column. Transference of stresses from the concrete component to the steel core takes place with shear studs welded on the steel section before the installation of the reinforcement, while additional dowels might be required for the longitudinal bars that are not adequately constrained by the installed stirrups. Nevertheless, all aforementioned do not affect the column's resistance to axial loading, or its flexural stiffness, so in this work the components taken into consideration are the I-shaped section, the concrete and the longitudinal reinforcement, as illustrated in Fig. 3.a.

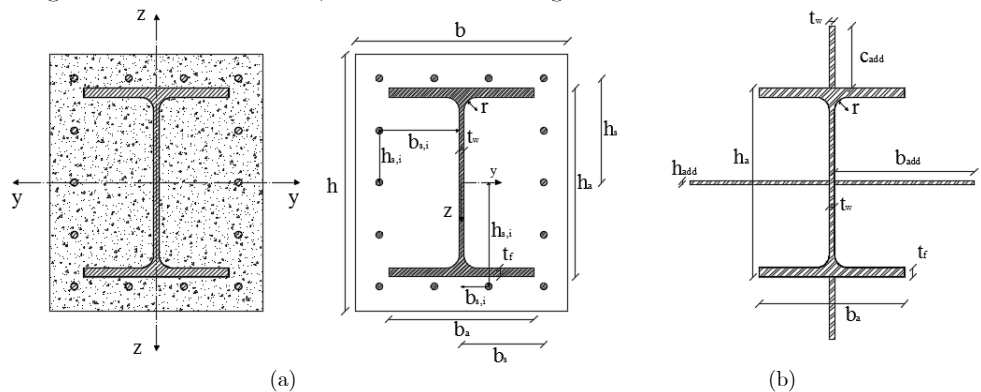


Figure 3. Geometric characteristics of the (a) composite concrete-encased and (b) fictitious pure-steel I-shaped section

Longitudinal reinforcement is installed so that it forms a rectangular cage. The same geometry was considered for the rectangular hollow sections, so the total area and combined second moment of area of the reinforcement are determined using Eqns. 3.1, 3.5 and 3.8. Regarding the steel I-shaped section, the same properties are calculated considering rectangular components and adding or subtracting their properties correspondingly. Two additional variables are defined for the dimensions of the hollow rectangles defined by the section's flanges and its web:  $b'_a = (b_a - t_w)/2$  and  $h'_a = h_a - 2 \cdot t_f$ . In order to simplify the resulting equations, normalized values are used in this Section as well (Eqns. 4.1 and 4.2).

- Normalized by the breadth of the composite section:

$$\frac{t_w}{b} = \theta, \quad \frac{b'_a}{b} = \beta_a \quad \text{and} \quad \frac{b'_a}{b} = \beta'_a \quad (4.1)$$

- Normalized by the height of the composite section:

$$\frac{t_w}{h} = \theta', \quad \frac{h_a}{h} = \eta_a \quad \text{and} \quad \frac{h'_a}{h} = \eta'_a \quad (4.2)$$

So, the total area of the steel I-shaped section (Eqn. 4.3) is calculated as the area of the surrounding rectangle, subtracting the area of the two hollow rectangles on both sides of the web. The same applies on the calculation of the second moment of area about the major axis (Eqn. 4.4), since the center of all aforementioned components is on y-axis. For the calculation of the second moment of area about the minor axis (Eqn. 4.5), three rectangles (*breadth* ; *height*) with the same center need to be considered: the external one ( $b$  ;  $h$ ), the one defined by the internal sides of the section's flanges ( $b$  ;  $h'_a$ ), and the web of the section between the two flanges ( $t_w$  ;  $h'_a$ ).

$$A_a = b_a \cdot h_a - 2 \cdot b'_a \cdot h'_a = \beta_a \cdot b \cdot \eta_a \cdot h - 2 \cdot \beta'_a \cdot b \cdot \eta'_a \cdot h \Rightarrow A_a = (\beta_a \cdot \eta_a - 2 \cdot \beta'_a \cdot \eta'_a) \cdot b \cdot h \quad (4.3)$$

$$I_{y,a} = \left( \frac{b_a \cdot h_a^3}{12} \right) - 2 \cdot \left( \frac{b'_a \cdot h'^3_a}{12} \right) \Rightarrow I_{y,a} = \left( \frac{\beta_a \cdot b \cdot \eta_a^3 \cdot h^3}{12} \right) - 2 \cdot \left( \frac{\beta'_a \cdot b \cdot \eta'^3_a \cdot h^3}{12} \right) \Rightarrow I_{y,a} = (\beta_a \cdot \eta_a^3 - 2 \cdot \beta'_a \cdot \eta'^3_a) \cdot \left( \frac{b \cdot h^3}{12} \right) \quad (4.4)$$

$$I_{z,a} = \left( \frac{b_a^3 \cdot h_a}{12} \right) - \left( \frac{b_a^3 \cdot h'_a}{12} \right) + \left( \frac{t_w^3 \cdot h'_a}{12} \right) \Rightarrow I_{z,a} = \left( \frac{\beta_a^3 \cdot b^3 \cdot \eta_a \cdot h}{12} \right) - \left( \frac{\beta_a^3 \cdot b^3 \cdot \eta'_a \cdot h}{12} \right) + \left( \frac{\theta^3 \cdot b^3 \cdot \eta'_a \cdot h}{12} \right) \Rightarrow I_{z,a} = (\beta_a^3 \cdot \eta_a - \beta_a^3 \cdot \eta'_a + \theta^3 \cdot \eta'_a) \cdot \left( \frac{b^3 \cdot h}{12} \right) \quad (4.5)$$

The concrete section has a particularly irregular shape, mainly due to the existence of the longitudinal reinforcement, so its geometrical properties (Eqns. 4.6, 4.7 and 4.8) are indirectly calculated by subtracting the ones corresponding to the steel core and the longitudinal reinforcement from those of the external rectangle ( $b$  ;  $h$ ).

$$A_c = b \cdot h - A_a - A_s = b \cdot h - (\beta_a \cdot \eta_a - 2 \cdot \beta'_a \cdot \eta'_a) \cdot b \cdot h - (2 \cdot n + 2 \cdot m - 4) \cdot \left( \frac{\pi \cdot d^2}{4} \right) \Rightarrow A_c = (1 - \beta_a \cdot \eta_a + 2 \cdot \beta'_a \cdot \eta'_a) \cdot b \cdot h - (2 \cdot n + 2 \cdot m - 4) \cdot \left( \frac{\pi \cdot d^2}{4} \right) \quad (4.6)$$

$$I_{y,c} = \left( \frac{b \cdot h^3}{12} \right) - I_{y,a} - I_{y,s} = \left( \frac{b \cdot h^3}{12} \right) - (\beta_a \cdot \eta_a^3 - 2 \cdot \beta'_a \cdot \eta'^3_a) \cdot \left( \frac{b \cdot h^3}{12} \right) - I_{y,s} \Rightarrow I_{y,c} = (1 - \beta_a \eta_a^3 + 2 \beta'_a \eta'^3_a) \cdot \left( \frac{b h^3}{12} \right) - \left( \frac{\pi d^2}{2} \right) \cdot \left[ (n + m - 2) \cdot \left( \frac{d^2}{16} \right) + m h_s^2 + \sum_{i=1}^{n-2} h_{s,i}^2 \right] \quad (4.7)$$

$$I_{z,c} = \left( \frac{b^3 \cdot h}{12} \right) - I_{z,a} - I_{z,s} = \left( \frac{b^3 \cdot h}{12} \right) - (\beta_a^3 \cdot \eta_a - \beta_a^3 \cdot \eta'_a + \theta^3 \cdot \eta'_a) \cdot \left( \frac{b^3 \cdot h}{12} \right) - I_{z,s} \Rightarrow I_{z,c} = (1 - \beta_a^3 \cdot \eta_a + \beta_a^3 \cdot \eta'_a - \theta^3 \cdot \eta'_a) \cdot \left( \frac{b^3 h}{12} \right) - \left( \frac{\pi d^2}{2} \right) \cdot \left[ (n + m - 2) \cdot \left( \frac{d^2}{16} \right) + n b_s^2 + \sum_{i=1}^{m-2} b_{s,i}^2 \right] \quad (4.8)$$

Using the normalized values  $\rho_a$ ,  $\rho_s$ ,  $\rho'_a$  and  $\rho'_s$  defined in Section 2, a more compact expression is determined for the area of the concrete (Eqn. 4.9).

$$A_a + A_c + A_s = b \cdot h \Rightarrow A_a + A_c + \rho_s \cdot A_c = b \cdot h \Rightarrow A_a + (1 + \rho_s) \cdot A_c = b \cdot h \Rightarrow$$

$$\begin{aligned} \rho_a \cdot b \cdot h + (1 + \rho_s) \cdot A_c &= b \cdot h \Rightarrow (1 + \rho_s) \cdot A_c = (1 - \rho_a) \cdot b \cdot h \Rightarrow \\ A_c &= \frac{(1 - \rho_a)}{(1 + \rho_s)} \cdot b \cdot h = \frac{\rho'_a}{\rho'_s} \cdot b \cdot h \end{aligned} \quad (4.9)$$

The fictitious pure-steel section selected is based on a similar method used for partially-encased I-shaped sections (47). It consists of the steel I-shaped section used in the composite section, reinforced by additional plates installed on its flanges and web, as illustrated in Fig. 3.b. The flange plates installed have the same thickness as the web of the steel section, while their height ( $d_{add}$ ), as well as the height ( $h_{add}$ ) and breadth ( $b_{add}$ ) of the web plates are variables.

The position of the plates was selected so that their centroids match those of the I-shaped section. The geometrical properties of the I-shaped section have already been calculated (Eqns. 4.3, 4.4 and 4.5), so only those of the additional plates (Eqns. 4.10, 4.11 and 4.12) need to be defined. The plates' dimensions are normalized by dividing with the breadth of the composite section ( $b_{add} = \beta \cdot b$  and  $t_w = \theta \cdot b$ ) and its height ( $h_{add} = \eta \cdot h$  and  $d_{add} = \chi \cdot h$ ).

$$A_{add} = 2 \cdot b_{add} \cdot h_{add} + 2 \cdot d_{add} \cdot t_w = 2 \cdot (\beta \cdot \eta + \chi \cdot \theta) \cdot b \cdot h \quad (4.10)$$

$$\begin{aligned} I_{y,add} &= 2 \cdot \frac{b_{add} \cdot h_{add}^3}{12} + \frac{t_w \cdot (2 \cdot c_{add} + h_a)^3}{12} - \frac{t_w \cdot h_a^3}{12} \Rightarrow \\ I_{y,add} &= \left( 2 \cdot \beta \cdot \eta^3 + \theta \cdot (2 \cdot \chi + \eta)^3 - \theta \cdot \eta^3 \right) \cdot \frac{b \cdot h^3}{12} \end{aligned} \quad (4.11)$$

$$\begin{aligned} I_{z,add} &= 2 \cdot \frac{t_w^3 \cdot d_{add}}{12} + \frac{(2 \cdot b_{add} + t_w)^3 \cdot h_{add}}{12} - \frac{t_w^3 \cdot h_{add}}{12} \Rightarrow \\ I_{z,add} &= \left( 2 \cdot \theta^3 \cdot \chi + (2 \cdot \beta + \theta)^3 \cdot \eta - \theta^3 \cdot \eta \right) \cdot \frac{b^3 \cdot h}{12} \end{aligned} \quad (4.12)$$

Applying the equilibrium of axial resistances, dividing by the yielding stress of structural steel and eliminating the area of the steel I-shaped section which appears on both sides of the equation, a relationship between the area of the plates and those of the concrete and the reinforcement is determined (Eqn. 4.13).

$$\begin{aligned} N_{Rd}^{fict} = N_{Rd}^{act} &\Rightarrow A_{fict} \cdot f_a = A_a \cdot f_a + A_c \cdot f_c + A_s \cdot f_s \Rightarrow \\ A_a \cdot f_a + A_{add} \cdot f_a &= A_a \cdot f_a + A_c \cdot f_c + A_s \cdot f_s \Rightarrow \\ A_{add} \cdot f_a &= A_c \cdot f_c + A_s \cdot f_s \end{aligned} \quad (4.13)$$

Substituting the areas of the plates (Eqn. 4.10), concrete (Eqn. 4.9) and reinforcing steel ( $A_s = \rho_s \cdot A_c$ ) in Eqn. 4.13 and dividing by  $b \cdot h$ , it transforms to a function between  $\beta$ ,  $\eta$  and  $\chi$  (Eqn. 4.14).

$$\begin{aligned} A_{add} \cdot f_a = A_c \cdot f_c + A_s \cdot f_s &\Rightarrow \frac{(2 \cdot b_{add} \cdot h_{add} + 2 \cdot c_{add} \cdot t_w) \cdot f_a}{f_a} = \frac{A_c \cdot f_c}{f_a} + \frac{A_s \cdot f_s}{f_a} \Rightarrow \\ 2 \cdot b_{add} \cdot h_{add} + 2 \cdot c_{add} \cdot t_w &= A_c \cdot \phi_c + A_s \cdot \phi_s \Rightarrow \\ \left( \frac{1}{b \cdot h} \right) \cdot (2 \cdot \beta \cdot b \cdot \eta \cdot h + 2 \cdot \chi \cdot h \cdot \theta \cdot b) &= \left( \frac{1}{b \cdot h} \right) \cdot \left( \frac{\rho'_a}{\rho'_s} \cdot b \cdot h \cdot \phi_c + \frac{\rho'_a}{\rho'_s} \cdot b \cdot h \cdot \rho_s \cdot \phi_s \right) \Rightarrow \\ (2 \cdot \beta \cdot \eta + 2 \cdot \chi \cdot \theta) &= \frac{\rho'_a}{\rho'_s} \cdot (\phi_c + \rho_s \cdot \phi_s) \end{aligned} \quad (4.14)$$

The second and third equations are determined by the equilibrium of flexural stiffness about the major and minor axis respectively. In order to simplify the final equations received, the ratios  $\alpha_{s,y}$  (Eqn. 3.30) and  $\alpha_{s,z}$  (Eqn. 3.32) are introduced. Where possible, the normalized values previously defined in this work are used. In both equations, the each component's geometrical properties are replaced with the expressions provided in (a) Eqns. 4.4, 4.7, 3.5 and 4.11 for the



second moment of area about the major axis and (b) Eqns. 4.5, 4.8, 3.8 and 4.12 for the second moment of area about the minor axis. Normalizing by  $b \cdot h^3 / 12$  and  $b^3 \cdot h / 12$  respectively, the resulting equations (Eqns. 4.15 and 4.16) are both functions of  $\beta$ ,  $\eta$  and  $\chi$ .

$$\begin{aligned}
 (E \cdot I)_{y, \text{fict}} &= (E \cdot I)_{y, \text{act}} \Rightarrow E_a \cdot I_{y, a} + E_a \cdot I_{y, \text{add}} = E_a \cdot I_{y, a} + E_c \cdot I_{y, c} + E_s \cdot I_{y, s} \Rightarrow \\
 E_a \cdot I_{y, \text{add}} &= E_c \cdot I_{y, c} + E_s \cdot I_{y, s} \Rightarrow \frac{E_a \cdot I_{y, \text{add}}}{E_a} = \frac{E_c \cdot I_{y, c}}{E_a} + \frac{E_s \cdot I_{y, s}}{E_a} \Rightarrow I_{y, \text{add}} = \psi_c \cdot I_{y, c} + \psi_s \cdot I_{y, s} \Rightarrow \\
 \left( \frac{2 \cdot \frac{b_{\text{add}} \cdot h_{\text{add}}^3}{12} + \frac{t_w \cdot (2 \cdot c_{\text{add}} + h_a)^3}{12} - \frac{t_w \cdot h_a^3}{12}}{\left( \frac{b \cdot h^3}{12} \right)} \right) &= \frac{\psi_c \cdot I_{y, c}}{\left( \frac{b \cdot h^3}{12} \right)} + \frac{\psi_s \cdot I_{y, s}}{\left( \frac{b \cdot h^3}{12} \right)} \Rightarrow \\
 2 \cdot \beta \cdot \eta^3 + \theta \cdot (2 \cdot \chi + \eta_a)^3 - \theta \cdot \eta_a^3 &= \psi_c \cdot \frac{I_{y, c}}{\left( \frac{b \cdot h^3}{12} \right)} + \psi_s \cdot \alpha_{s, y} \Rightarrow \\
 2 \cdot \beta \cdot \eta^3 + \theta \cdot (2 \cdot \chi + \eta_a)^3 - \theta \cdot \eta_a^3 &= \psi_c \cdot \frac{(1 - \beta_a \eta_a^3 - 2\beta'_a \eta'_a{}^3) \cdot \left( \frac{bh^3}{12} \right) - I_{y, s}}{\left( \frac{b \cdot h^3}{12} \right)} + \psi_s \cdot \alpha_{s, y} \Rightarrow \\
 2 \cdot \beta \cdot \eta^3 + \theta \cdot (2 \cdot \chi + \eta_a)^3 - \theta \cdot \eta_a^3 &= \psi_c \cdot (1 - \beta_a \eta_a^3 - 2\beta'_a \eta'_a{}^3) + (\psi_s - \psi_c) \cdot \alpha_{s, y} \quad (4.15)
 \end{aligned}$$

$$\begin{aligned}
 E_a \cdot I_{z, \text{add}} &= E_c \cdot I_{z, c} + E_s \cdot I_{z, s} \Rightarrow \frac{E_a \cdot I_{z, \text{add}}}{E_a} = \frac{E_c \cdot I_{z, c}}{E_a} + \frac{E_s \cdot I_{z, s}}{E_a} \Rightarrow \\
 I_{z, \text{add}} &= \psi_c \cdot I_{z, c} + \psi_s \cdot I_{z, s} \Rightarrow \frac{I_{z, \text{add}}}{\frac{b^3 \cdot h}{12}} = \frac{\psi_c \cdot I_{z, c}}{\frac{b^3 \cdot h}{12}} + \frac{\psi_s \cdot I_{z, s}}{\frac{b^3 \cdot h}{12}} \Rightarrow \\
 \frac{2 \cdot \frac{t_w^3 \cdot c_{\text{add}}}{12} + \frac{(2 \cdot b_{\text{add}} + t_w)^2 \cdot h_{\text{add}}}{12} - \frac{t_w^3 \cdot h_{\text{add}}}{12}}{\frac{b^3 \cdot h}{12}} &= \psi_c \cdot \frac{I_{z, c}}{\frac{b^3 \cdot h}{12}} + \psi_s \cdot a_{s, z} \Rightarrow \\
 2 \cdot \theta^3 \cdot \chi + (2 \cdot \beta + \theta)^2 \cdot \eta - \theta^3 \cdot \eta &= \psi_c \cdot \frac{(1 - \beta_a^3 \eta_a - 2\beta'_a{}^3 \eta'_a) \cdot \left( \frac{b^3 h}{12} \right) - I_{z, s}}{\frac{b^3 \cdot h}{12}} + \psi_s \cdot a_{s, z} \Rightarrow \\
 2 \cdot \theta^3 \cdot \chi + (2 \cdot \beta + \theta)^2 \cdot \eta - \theta^3 \cdot \eta &= \psi_c \cdot (1 - \beta_a^3 \eta_a - 2\beta'_a{}^3 \eta'_a) + (\psi_s - \psi_c) \cdot a_{s, z} \quad (4.16)
 \end{aligned}$$

Since the expressions on the left side of Eqns. 4.14, 4.15 and 4.16 are positive numbers, while all variables on the right side of the equations have known values, the latter are replaced by the positive known variables  $d_x^2$ ,  $d_y^2$  and  $d_z^2$ . It should be noted that the aforementioned should not be confused with those defined in Sections 2 and 3. Hence, Eqns. 4.14, 4.15 and 4.16 transform into the following:

$$2 \cdot \beta \cdot \eta + 2 \cdot \chi \cdot \theta = d_x^2 \quad (4.17)$$

$$2 \cdot \beta \cdot \eta^3 + \theta \cdot (2 \cdot \chi + \eta_a)^3 = d_y^2 \quad (4.18)$$

$$2 \cdot \theta^3 \cdot \chi + (2 \cdot \beta + \theta)^2 \cdot \eta - \theta^3 \cdot \eta = d_z^2 \quad (4.19)$$

Three additional variables are defined, in order to perform the required operations on Eqns. 4.17, 4.18 and 4.19 and solve for the unknown variables  $\beta$ ,  $\eta$  and  $\chi$ :  $\mu_x = \eta_a + d_x^2 / \theta$ ,  $\mu_y = \sqrt[3]{\eta_a^3 + d_y^2 / \theta}$  and  $\mu_z = \eta_a + d_z^2 / \theta$ . Eqn. 4.17

is divided by  $\vartheta$  and Eqns. 4.18 and 4.19 are divided by  $\vartheta^3$ , so Eqns. 4.20, 4.21 and 4.22 are formulated.

$$2 \cdot \beta \cdot (\eta/\theta) + 2 \cdot \chi = d_x^2/\theta \Rightarrow 2 \cdot \beta \cdot (\eta/\theta) + 2 \cdot \chi = \mu_x - \eta_a \quad (4.20)$$

$$2 \cdot \beta \cdot (\eta/\theta)^3 \cdot \theta^2 + (2 \cdot \chi + \eta_a)^3 - \eta_a^3 = d_y^2/\theta \Rightarrow$$

$$2 \cdot \beta \cdot (\eta/\theta)^3 \cdot \theta^2 + (2 \cdot \chi + \eta_a)^3 = \eta_a^3 + d_y^2/\theta \Rightarrow$$

$$2 \cdot \beta \cdot (\eta/\theta)^3 \cdot \theta^2 + (2 \cdot \chi + \eta_a)^3 = \mu_y^3 \quad (4.21)$$

$$2 \cdot \chi + (2 \cdot \beta + \theta)^3 \cdot \eta/\theta^3 - \eta = d_z^2/\theta^3 \Rightarrow \quad (4.22)$$

$$2 \cdot \chi + ((2 \cdot \beta + \theta)^3 - 1) \cdot (\eta/\theta)/\theta^2 = \mu_z - \eta_a$$

The product  $2 \cdot \beta \cdot (\eta/\theta)^3 \cdot \theta^2$  in Eqn. 4.21 is particularly smaller than the others, so it may be omitted without significant effect on the final outcome. So, eliminating  $2 \cdot \beta \cdot (\eta/\theta)^3 \cdot \theta^2$  from the equation, the unknown variable  $\chi$  is determined.

$$(2 \cdot \chi + \eta_a)^3 \approx \mu_y^3 \Rightarrow (2 \cdot \chi + \eta_a) \approx \mu_y \Rightarrow (2 \cdot \chi) \approx \mu_y - \eta_a \Rightarrow \chi \approx (\mu_y - \eta_a)/2 \quad (4.23)$$

Substituting  $2 \cdot \chi$  from Eqn. 4.23 in Eqn. 4.20, a function between  $\beta$  and  $\eta$  is received:

$$2 \cdot \beta \cdot (\eta/\theta) + \mu_y - \eta_a \approx \mu_x - \eta_a \Rightarrow 2 \cdot \beta \cdot (\eta/\theta) \approx \mu_x - \mu_y \quad (4.24)$$

The values of  $2 \cdot \chi$  and  $2 \cdot \beta \cdot (\eta/\theta)$ , defined in Eqns. 4.23 and 4.24 respectively, are introduced in Eqn. 4.22, so a function of  $\beta$  is determined.

$$\mu_y - \eta_a + ((2 \cdot \beta + \theta)^3 - 1) \cdot (\eta/\theta)/\theta^2 \approx \mu_z - \eta_a \Rightarrow$$

$$((2 \cdot \beta + \theta)^3 - 1) \cdot (\eta/\theta)/\theta^2 \approx \mu_z - \mu_y \Rightarrow$$

$$\left(\frac{2 \cdot \beta}{\theta}\right)^2 + 3 \cdot \left(\frac{2 \cdot \beta}{\theta}\right) + 3 \approx \frac{\mu_z - \mu_y}{\mu_x - \mu_y} \Rightarrow$$

$$\left(\frac{2 \cdot \beta}{\theta}\right)^2 + 3 \cdot \left(\frac{2 \cdot \beta}{\theta}\right) + \left(3 - \frac{\mu_z - \mu_y}{\mu_x - \mu_y}\right) \approx 0 \quad (4.25)$$

Eqn. 4.25 is a quadratic equation in which the unknown variable is  $(2 \cdot \beta/\theta)$ . Since both its numerator and denominator are positive numbers, only the positive solution of the equation is valid. So, solving for  $\beta$ , its value is determined in Eqn. 4.26.

$$\left(\frac{2 \cdot \beta}{\theta}\right) \approx \sqrt{\frac{\mu_z - \mu_y}{\mu_x - \mu_y} - \frac{3}{4}} - \frac{3}{2} = \frac{\sqrt{4 \cdot (\mu_z - \mu_y) - 3 \cdot (\mu_x - \mu_y)} - 3 \cdot \sqrt{\mu_x - \mu_y}}{2 \cdot \sqrt{\mu_x - \mu_y}} \Rightarrow$$

$$\beta \approx \left(\frac{\theta}{2}\right) \cdot \left(\sqrt{\frac{\mu_z - \mu_y}{\mu_x - \mu_y} - 0.75} - 1.5\right) \Rightarrow$$

$$\beta \approx \theta \cdot \frac{\sqrt{4 \cdot (\mu_z - \mu_y) - 3 \cdot (\mu_x - \mu_y)} - 3 \cdot \sqrt{\mu_x - \mu_y}}{4 \cdot \sqrt{\mu_x - \mu_y}} \quad (4.26)$$

The unknown variable  $\eta$  is defined by dividing  $(2 \cdot \beta) \cdot (\eta/\theta)$  by  $(2 \cdot \beta/\theta)$ , using the expressions provided in Eqns. 4.24 and 4.26 respectively.

$$\eta = \frac{(2 \cdot \beta) \cdot (\eta/\theta)}{(2 \cdot \beta/\theta)} \Rightarrow \eta \approx \frac{(\mu_x - \mu_y) \cdot 2 \cdot \sqrt{\mu_x - \mu_y}}{\sqrt{4 \cdot (\mu_z - \mu_y) - 3 \cdot (\mu_x - \mu_y)} - 3 \cdot \sqrt{\mu_x - \mu_y}} \Rightarrow$$

$$\eta \approx \frac{2 \cdot \sqrt{\mu_x - \mu_y}^3}{\sqrt{4 \cdot (\mu_z - \mu_y) - 3 \cdot (\mu_x - \mu_y) - 3 \cdot \sqrt{\mu_x - \mu_y}}} \quad (4.27)$$

Finally, the dimensions of the installed plates on the fictitious pure-steel section are provided in Eqns. 4.28, 4.29 and 4.30:

$$b_{add} = \beta \cdot b = \left( \theta \cdot \frac{\sqrt{4 \cdot (\mu_z - \mu_y) - 3 \cdot (\mu_x - \mu_y) - 3 \cdot \sqrt{\mu_x - \mu_y}}}{4 \cdot \sqrt{\mu_x - \mu_y}} \right) \cdot b \quad (4.28)$$

$$h_{add} = \eta \cdot h = \left( \frac{2 \cdot \sqrt{\mu_x - \mu_y}^3}{\sqrt{4 \cdot (\mu_z - \mu_y) - 3 \cdot (\mu_x - \mu_y) - 3 \cdot \sqrt{\mu_x - \mu_y}}} \right) \cdot h \quad (4.29)$$

$$d_{add} \Rightarrow \chi \cdot h = \left( \frac{\mu_y - \eta_a}{2} \right) \cdot h \quad (4.30)$$

### Assessment of the simulation method

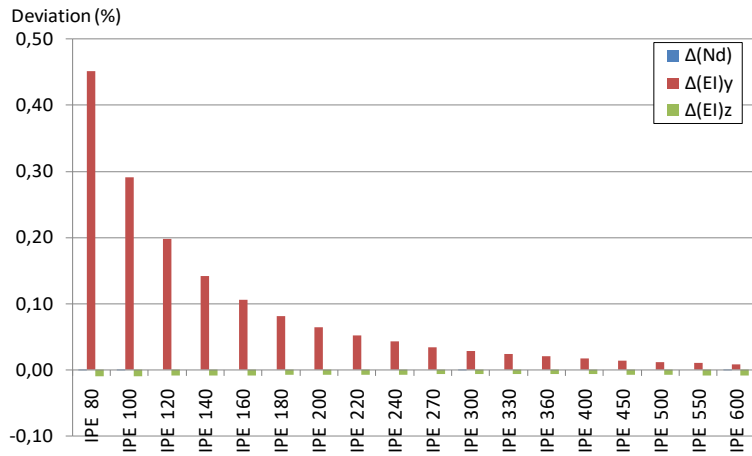
Since a simplification was made in order to define the solution of the set of Eqns. 4.17, 4.18 and 4.19, resulting in the removal of the component  $2 \cdot \beta \cdot (\eta/\theta)^3 \cdot \theta^2$  in Eqn. 4.21, the formulas determined are not in a closed form, and so they provide an approximate value for each variable. Hence, the accuracy of the simulation formulas needs to be evaluated. For this purpose, a variety of standard I-shaped sections were selected. As a reference, a typical concrete-encased composite column section consisting of a HE320A steel core is used. The concrete compressive strength is 25MPa (*i.e.* C25/30 grade), while its cover on all sides of the column is 50mm from the rectangle defined by the steel section's flanges. Its linear reinforcement consists of 12mm diameter bars, the yielding stress of which is 500MPa. A total number of 12 bars are installed: 5 bars parallel to the column's height and 3 bars parallel to its breadth. Eqns. 4.31, 4.32 and 4.33 provide the formulas to calculate the deviation of the composite section's axial capacity (Eqn. 4.31) and flexural stiffness about the major and minor axis (Eqns. 4.31 and 4.32 respectively).

$$\Delta(Nd) = \frac{N_{Rd,act} - N_{Rd,fict}}{N_{Rd,act}} = \frac{(f_a \cdot A_a + f_c \cdot A_c + f_s \cdot A_s) - f_a \cdot A_{fict}}{(f_a \cdot A_a + f_c \cdot A_c + f_s \cdot A_s)} \quad (4.31)$$

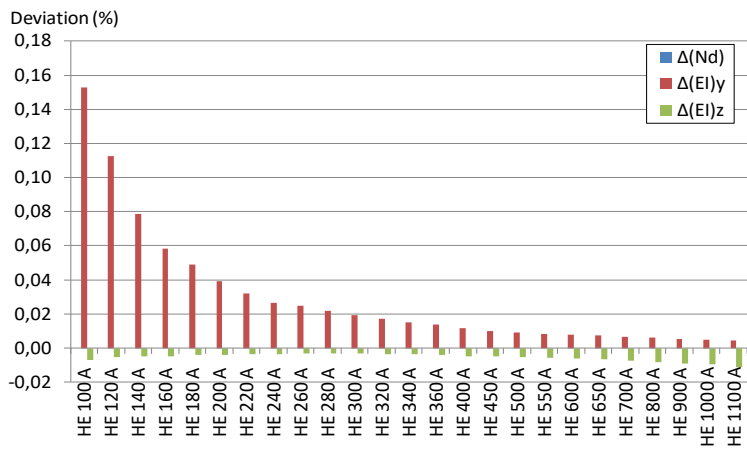
$$\Delta(EI)_y = \frac{EI_{tot,y,act} - E_a \cdot I_{y,fict}}{EI_{tot,y,act}} = \frac{(E_a \cdot I_{y,a} + E_c \cdot I_{y,c} + E_s \cdot I_{y,s}) - E_a \cdot I_{y,fict}}{(E_a \cdot I_{y,a} + E_c \cdot I_{y,c} + E_s \cdot I_{y,s})} \quad (4.32)$$

$$\Delta(EI)_z = \frac{EI_{tot,z,act} - E_a \cdot I_{z,fict}}{EI_{tot,z,act}} = \frac{(E_a \cdot I_{z,a} + E_c \cdot I_{z,c} + E_s \cdot I_{z,s}) - E_a \cdot I_{z,fict}}{(E_a \cdot I_{z,a} + E_c \cdot I_{z,c} + E_s \cdot I_{z,s})} \quad (4.33)$$

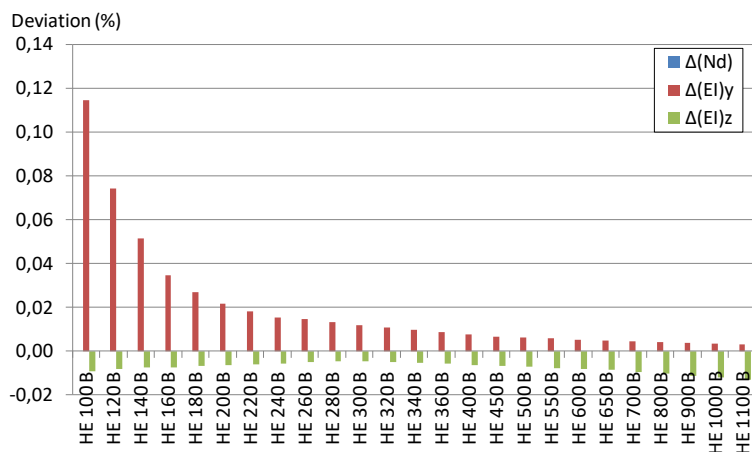
The proposed simulation method was applied and the fictitious section's axial capacity and flexural stiffness were calculated. Comparing the aforementioned with the properties of the composite section, the largest deviation is noticed on the stiffness about the major axis, *i.e.* 0.021%. In engineering practice, an admissible deviation level would be less than 5%, while for values less than 1% the method would be considered to have high accuracy. The determined values are particularly smaller than the aforementioned high accuracy limit, so one could consider the steel-concrete composite section and the fictitious pure-steel section to have practically the same properties. In order to evaluate the proposed method and to determine the limitations that might apply, a



(a)



(b)



(c)

Figure 4. Assessment of the accuracy of the simulation method: (a) IPE, (b) HEA, (c) HEB sections.

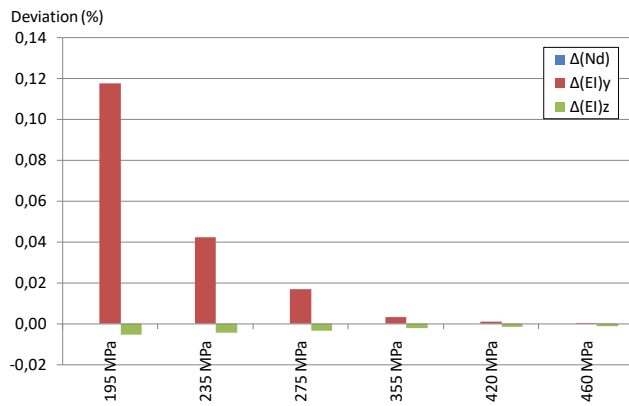


Figure 5. Assessment of the accuracy of the simulation method: Structural steel grade.

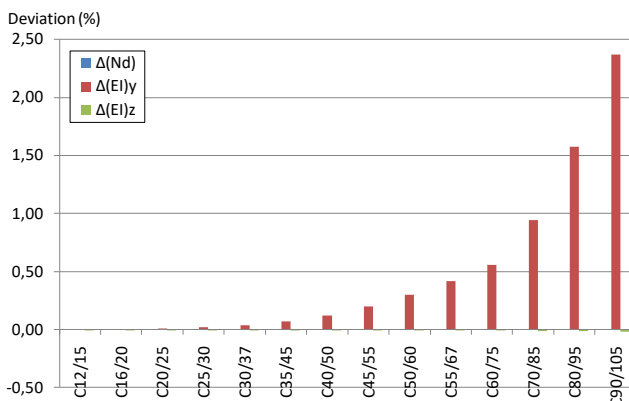


Figure 6. Assessment of the accuracy of the simulation method: Concrete strength class.

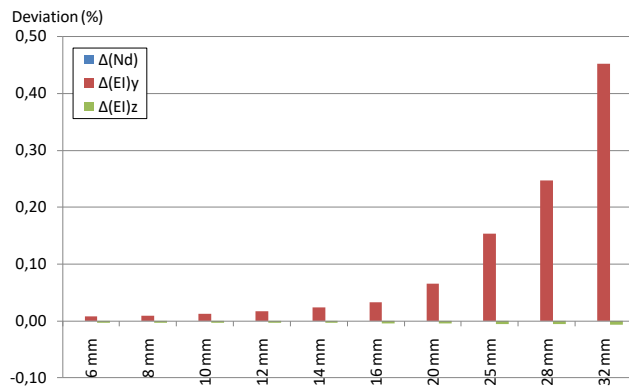


Figure 7. Assessment of the accuracy of the simulation method: Rebar diameter.

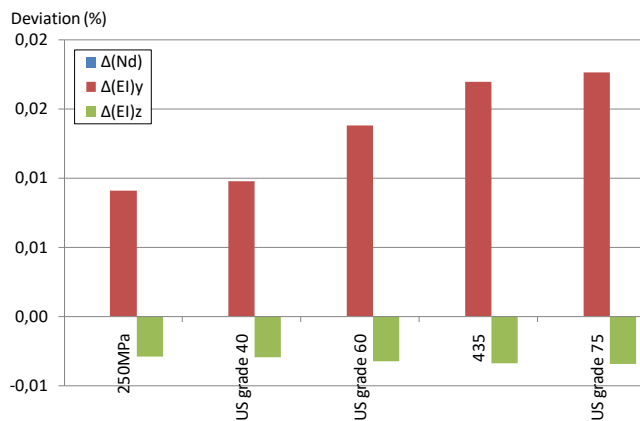


Figure 8. Assessment of the accuracy of the simulation method: Reinforcing steel grade.

thorough investigation on the factors which affect its accuracy needs to take place. Hence, a total number of 101 simulations were performed. The factors taken into consideration are: (a) the core I-shaped steel section, (b) the structural steel yielding stress, (c) the concrete strength, (d) the rebar diameter and (e) the reinforcing steel yielding stress.

In order to determine the effect of the steel core size on the accuracy of the proposed simulation method, three sets of standard I-shaped sections were considered: (a) 18 IPE sections with sizes from IPE80 to IPE600, (b) 25 HEA sections with sizes from HE100A to HE1100A and (c) 25 HEB sections with sizes from HE100B to HE1100B. It should be noted that typically HEA and HEB sections are preferred for steel or composite columns, while IPE sections are mainly used as beam sections. So their use in this work is mainly for investigation purpose. The fictitious section properties were compared to those of the actual composite sections and the results are illustrated in Figs. 4.a, 4.b and 4.c for the IPE, HEA and HEB sections respectively. For all sections it is noticed that there is no deviation between the axial capacity of the actual and the defined fictitious section. Furthermore, the deviation on the section's stiffness about the minor axis is in all cases negative. Compared to the deviation on the section's stiffness about its major axis, it is particularly smaller. Its minimum absolute value is 0.002% and its maximum value is 0.0149%. In all scenarios it can be assumed negligible, as it is less than the deviation that occurs for a composite column simulated using fiber element model with a large number of fibers for each component and a simple model using the minimum admissible number of fibers.

The range of values of deviation on the stiffness about the major axis is significantly larger. In all cases it is positive and it was calculated from 0.0041% up to 0.5434%. It should be noted that the largest values are found for the smaller sections of each group (IPE80-IPE100, HE100A and HE100B). Steel sections with height less than 200mm are typically not used in engineering practice as core for concrete-encased composite sections, as there is not enough space on its web for the installation of the required shear headed studs, in order to achieve the composite performance of the column. For larger section sizes, the deviation is particularly decreased with the maximum value being less than 0.1% (it is determined for IPE200). In all Figs. it can be noticed that the larger the size of the core section is, the more the deviation decreases. In order to verify this correlation, one needs to examine the stiffness percentage provided to the column section by the steel core. Fig. 9 illustrates the total stiffness contribution of (a) the steel core and (b) the reinforced concrete to the composite section. It can be noticed that for small sizes the contribution of the steel core is particularly lower than that of the reinforced concrete: IPE80 section provides only 5.78% of the composite section's stiffness, so it could be considered as a practically reinforced concrete section. For larger sections this is reversed and it reaches up to 53%. However, even though the stiffness of the steel core is taken into consideration on both the composite and the fictitious section, the additional plates simulate the reinforced concrete only. So, the deviation to the total stiffness about the major axis is directly related to the contribution of the reinforced concrete.

Similar effect to the accuracy of the simulation method was found to have the structural steel yielding stress. Even though it does not affect directly the overall stiffness of the composite or the fictitious section, but only their axial resistance, increased yielding stress was found to lead to reduced deviation on the stiffness about the major and minor axis. In particular, 6 steel grades with yielding stress from 195MPa to 460MPa (49) were considered and the results are presented in Fig. 5. In all cases there was no deviation on the axial capacity of

the sections, while the highest deviation for the stiffness about its minor axis was as low as 0.005%. The stiffness about the major axis reaches up to 0.118% for  $f_{y,a} = 195\text{MPa}$ , while there is no deviation for yielding stress higher than 460MPa. It should be noted that structural steel with yielding stress below 235MPa is currently not used in practice. The most common steel grades for normal capacity carbon steel are 275MPa and 355 MPa.

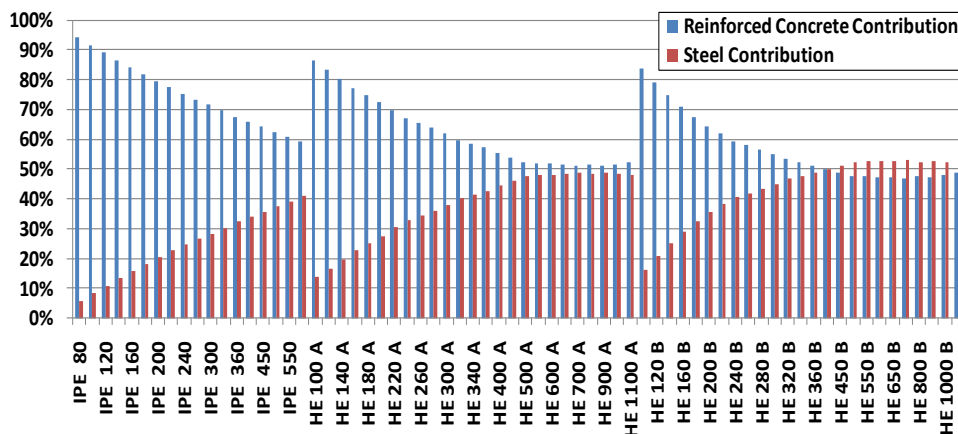


Figure 9. Contribution of the constituent materials (steel I-shaped core and surrounding reinforced concrete) to the total effective stiffness  $(EI)_{\text{eff}}$  of each composite column.

High grades of steel ( $f_{y,a} > 500\text{MPa}$ ) were also considered, but the results are not presented, as they do not provide additional information. In particular, for yielding stress higher than 355MPa the deviation is below 0.003%, while for 460MPa or higher there is no deviation. However, a remark made applying the proposed method for  $f_{y,a} = 800\text{MPa}$  was that the method could not yield results. The problem occurs on the calculation of the normalized value  $\beta$ . The calculation formula for  $\beta$  contains  $(\mu_x - \mu_y)$  as a denominator. Since  $\mu_z^3$  is a positive number, the product of  $(\mu_x - \mu_y)$  should be positive as well. The larger the value of  $f_{y,a}$  is, the smaller the normalized value  $\mu_x$  becomes, while  $\mu_y$  is not affected. No problem occurred when increased concrete strength was assumed. So, for particularly increased structural steel yielding stress, very low concrete strength classes cannot be used. However, the same applies in engineering practice already. The concrete strength is directly related to the structural steel yielding stress. As the stresses are transferred between the steel core and the concrete by the means of shear headed studs installed on the core section’s web, the lower the concrete strength is, the larger the number and diameter of the studs is required. So, high grade steel is typically used in cooperation with high strength concrete. Therefore, even though the aforementioned limitation applies on the proposed method mathematically, it is highly unlikely that such an issue might occur during its application in practice.

The investigated factor with the strongest effect on the accuracy of the simulation method is the concrete strength. A total number of 14 concrete strength classes were taken into consideration, from C12/15 up to C90/105 (50). It should be noted that concrete with strength less than 20MPa is typically not used for reinforced concrete or composite steel-concrete columns. Furthermore, concrete with strength equal to or more than 50MPa is classified as high-strength concrete (51). The results yielded are illustrated in Fig. 6. While, for low strength concrete classes the deviation is as low as 0.001%, for high-strength concrete, it increases dramatically, reaching up to 2.370%. This is a result of the increased contribution of the concrete to the stiffness of the composite section. The

concrete strength is directly related only to the section's axial resistance, on which there is no deviation in all investigated cases. However, increased concrete strength results in increased modulus of elasticity of the concrete as well (50). While C12/15 has a modulus of elasticity of 27GPa, it increases up to 44GPa for C90/105. Contrary to the contribution of the steel section investigated previously, that of reinforced concrete increases up to 63.74% for C50/60, but then drops down to 60.64% for C90/105. Hence, it can be assumed that the concrete's strength and its modulus of elasticity affect the results not only directly due to the properties of the composite section, but also through the normalized variables used.

The composite section's stiffness is also related to the reinforcing steel yielding stress, as well as the diameter of the installed bars. In order to investigate their effect on the accuracy of the proposed method, two more sets of simulations took place. In the first set, 10 bar diameters were used, ranging from 6mm to 32mm. In all cases there was found to be no deviation in the simulation of the axial resistance. The maximum deviation on the section's stiffness about both minor axes was found for the largest bar size used *i.e.* 32mm:  $\Delta(EI)_y = 0.453\%$  and  $\Delta(EI)_z = -0.006\%$ . Evaluation of the results illustrated in Fig. 7 shows that the deviation on the calculated stiffness dramatically for the larger bar sizes. This is directly related to the proportion of the section's stiffness provided by the longitudinal reinforcement, which increases with a similar rate. It is the combination of the rebars' location in relation to section's centroid and the elasticity modulus of the steel. In particular, for 6mm bars considered the proportion of the total stiffness about the major axis provided by the reinforcement is below 1%, while for the largest size considered, *i.e.* 32mm, it reaches up to 44%. In the second set, 5 steel grades were considered: from 250MPa to 517MPa (US grade 75) and the results yielded are presented in Fig. 8. It can be noticed that higher steel grades are associated with increased deviation on the section's stiffness. However, unlike the bar diameter, the effect of the steel yielding stress seems to have a linear correlation to the calculated deviation. It is also remarkable that, even though  $\Delta(EI)_y$  is particularly low,  $\Delta(EI)_z$  is not also reduced; its value is constantly -0.003%. Hence, it should be pointed out that, even though the ratio of  $\Delta(EI)_z$  over  $\Delta(EI)_y$  is particularly increased, the value of both is extremely low.

The applicability of the proposed method on reinforced concrete sections was also investigated. Because the functions of the variables  $\mu_x$ ,  $\mu_y$  and  $\mu_z$  required for the determination of the dimensions of the fictitious section contain components divided by  $\vartheta$ , the particular variable cannot be equal to zero. Hence, a fictitious composite section with a steel core without area or stiffness, but for which the variable  $\vartheta$  is equal to  $10^{-77}$  was considered. The value  $10^{-77}$  was not selected arbitrarily, but it is the smallest value for which the calculations can be performed in the software used. The materials comprising the fictitious section have the same properties as those used for the reference section, including the structural steel which is not installed. Finally, its height was considered to be 300mm and its breadth 200mm. Applying the proposed simulation method, it was noticed that while there is no deviation for the axial capacity and the stiffness about the minor axis, the calculated stiffness about the major axis is totally erroneous: its deviation reaches -99.515%. Various alternatives were also evaluated in order to improve the results to a deviation below the admissible limit, but all were unsuccessful. Hence, it can be assumed that the proposed method cannot be applied on reinforced concrete columns. Nevertheless, as the methods proposed in Sections 3 and 2 are mathematical functions of closed form,



a reinforced concrete column can alternatively be simulated as a pure-steel rectangular or circular hollow section.

## Concluding remarks

In this work, three methods were proposed in order to simulate steel-concrete composite columns with equivalent pure-steel columns. All methods intend to determine pure-steel sections which have the same axial resistance and stiffness about the major and minor axis as the composite steel-concrete section simulated. The methods outlined define fictitious hollow circular and rectangular pure-steel sections are in a closed form. Hence, the results yielded from their application define steel sections with exactly the same properties as their composite steel-concrete counterparts.

Formulas are provided regarding the calculation of the properties of the composite sections, but for standard sections such data can be retrieved directly from section tables and be normalized appropriately in order to calculate the variables  $d_x^2$ ,  $d_y^2$  and  $d_z^2$  when they are required. The formulas provided for the calculation of known variables, such as  $d_x^2$ ,  $d_y^2$  and  $d_z^2$ , as well as unknown variables, *i.e.*  $\alpha$ ,  $\beta$ ,  $\eta$ ,  $\chi$  and  $\gamma$ , use normalized values. So, the application of the proposed methods is independent of the measurement units used, while it is possible to scale the results (e.g. define a section with 1.5 times the stiffness about the minor axis) simply by multiplying  $d_x^2$ ,  $d_y^2$  and  $d_z^2$  with the required factor.

It is remarkable that both methods proposed for hollow sections are applicable on any type of section (e.g. reinforced concrete section). However, the same does not apply for the simulation method presented for I-shaped sections, which requires the existence of such a section in the core of the initial section, in order to yield accurate results. Nevertheless, the method is applicable with high accuracy for any concrete-encased I-shaped section, the construction of which is feasible in practice as well.

Application of the proposed simulation methods on sections with simpler geometry than the ones proposed, *i.e.* square hollow sections instead of rectangular sections and partially-encased I-shaped sections instead of “fully”-encased sections is possible. The formulas provided could be easily simplified, but this is not presented in this work, as it does not provide additional information. The proposed methods could also be generalized in order to simulate column sections with any type of materials. Additionally, the sections consisting of a single material (in this work it is steel), could consist of other materials, provided that the yielding stress ( $f_y$ ) and Young’s modulus ( $E_s$ ) are replaced by the respective values used in order to define the axial resistance and flexural stiffness of the alternative material accordingly. Nevertheless, when such an application takes place, the investigator should take into consideration all the differences between the materials on the actual sections and the simulated ones.

This work is not intended as an alternative to EC4, but as an additional tool for engineers in practice, so phenomena such as the various buckling types should be addressed according to the applicable design codes. Of particular importance is also that all proposed methods simulate the elastic behavior of the column sections. They can be applied for design purposes, in order to evaluate alternative solutions, or reduce the computational time required, especially when time-demanding procedures such as structural design optimization take place (52-56). However, the inelastic behavior of the composite section and its equivalent pure-

steel counterpart are not the same. Hence, the proposed methods cannot be applied in order to evaluate the inelastic performance of a building e.g. under a seismic excitation.

The post-elastic behavior of the sections depends mainly on their mechanical properties, while the formulas used consider a linear behavior up to the maximum stress/strain. Application of the described procedure in order to define a similar model in order that simulates the section's post-elastic behavior would be impractical, as one would need to define a different equivalent section for each step of the analysis, in order to achieve an acceptable level of accuracy of the simulation. A different approach than the one described in this work might be more suitable for this purpose.

## References

1. Gardner NJ, Jacobson ER. Structural behavior of concrete filled steel tubes. In *Journal Proceedings*. 1967;64(7): 404-413.
2. O'Shea MD, Bridge RQ. Design of circular thin-walled concrete filled steel tubes. *Journal of Structural Engineering*. 2000;126(11): 1295-1303.
3. Xiong DX, Zha XX. A numerical investigation on the behaviour of concrete-filled steel tubular columns under initial stresses. *Journal of Constructional Steel Research*. 2007;63(5): 599-611.
4. Lai MH, Ho JCM. A theoretical axial stress-strain model for circular concrete-filled-steel-tube columns. *Engineering Structures*. 2016;125: 124-143.
5. Zeghiche J, Chaoui K. An experimental behaviour of concrete-filled steel tubular columns. *Journal of Constructional Steel Research*. 2005;61(1): 53-66.
6. Brauns J. Analysis of stress state in concrete-filled steel column. *Journal of constructional steel research*. 1999;49(2): 189-196.
7. Kwan AKH, Dong CX, Ho JCM. Axial and lateral stress-strain model for concrete-filled steel tubes. *Journal of Constructional Steel Research*. 2016;122: 421-433.
8. Giakoumelis G, Lam D. Axial capacity of circular concrete-filled tube columns. *Journal of Constructional Steel Research*. 2004;60(7): 1049-1068.
9. Guo L, Zhang S, Kim WJ, Ranzi G. Behavior of square hollow steel tubes and steel tubes filled with concrete. *Thin-Walled Structures*. 2007;45(12): 961-973.
10. Ellobody E, Young B, Lam D. Behaviour of normal and high strength concrete-filled compact steel tube circular stub columns. *Journal of Constructional Steel Research*. 2006;62(7): 706-715.
11. Han LH, Yang, YF. Cyclic performance of concrete-filled steel CHS columns under flexural loading. *Journal of Constructional Steel Research*. 2005;61(4): 423-452.
12. Gupta PK, Sarda SM, Kumar MS. Experimental and computational study of concrete filled steel tubular columns under axial loads. *Journal of Constructional Steel Research*. 2007;63(2): 182-193.
13. Liang QQ, Fragomeni S. Nonlinear analysis of circular concrete-filled steel tubular short columns under eccentric loading. *Journal of Constructional Steel Research*. 2010;66(2): 159-169.
14. Lu ZH, Zhao YG. Suggested empirical models for the axial capacity of circular CFT stub columns. *Journal of Constructional Steel Research*. 2010;66(6): 850-862.
15. Zhu L, Ma L, Bai Y, Li S, Song Q, Wei Y, Sha X. Large diameter concrete-filled high strength steel tubular stub columns under compression. *Thin-Walled Structures*. 2016;108: 12-19.
16. Boyd PF, Cofer WF, Mclean DI. Seismic performance of steel-encased concrete columns under flexural loading. *ACI Structural Journal*. 1995;92(3): 355-364.
17. Liu D, Gho WM. Axial load behaviour of high-strength rectangular concrete-filled steel tubular stub columns. *Thin-Walled Structures*. 2005;43(8): 1131-1142.
18. Liu D. Behaviour of high strength rectangular concrete-filled steel hollow section columns under eccentric loading. *Thin-walled structures*. 2004;42(12): 1631-1644.
19. Lam D, Williams CA. Experimental study on concrete filled square hollow sections. *Steel and Composite Structures*. 2004;4(2): 95-112.
20. Shanmugam NE, Lakshmi B, Uy B. An analytical model for thin-walled steel box columns with concrete in-fill. *Engineering Structures*. 2002;24(6): 825-838.
21. Gramblicka S, Lelkes A. Analysis of composite steel-concrete columns. *Procedia Engineering*. 2012;40: 247-252.
22. Chitawadagi MV, Narasimhan MC, Kulkarni SM. Axial capacity of rectangular concrete-filled steel tube columns—DOE approach. *Construction and Building Materials*. 2010;24(4): 585-595.
23. Young B, Ellobody E. Experimental investigation of concrete-filled cold-formed high strength stainless steel tube columns. *Journal of Constructional Steel Research*. 2006;62(5): 484-492.

24. Lue DM, Liu JL, Yen T. Experimental study on rectangular CFT columns with high-strength concrete. *Journal of Constructional Steel Research*. 2007;63(1): 37-44.
25. Tao Z, Uy B, Liao FY, Han LH. Nonlinear analysis of concrete-filled square stainless steel stub columns under axial compression. *Journal of Constructional Steel Research*. 2011;67(11): 1719-1732.
26. Liu D. Tests on high-strength rectangular concrete-filled steel hollow section stub columns. *Journal of Constructional Steel Research*. 2005;61(7): 902-911.
27. Han LH. Tests on stub columns of concrete-filled RHS sections. *Journal of Constructional Steel Research*. 2002;58(3): 353-372.
28. Liu D, Gho WM, Yuan J. Ultimate capacity of high-strength rectangular concrete-filled steel hollow section stub columns. *Journal of Constructional Steel Research*. 2003;59(12): 1499-1515.
29. Han LH, Liu W, Yang YF. Behaviour of concrete-filled steel tubular stub columns subjected to axially local compression. *Journal of Constructional Steel Research*. 2008;64(4): 377-387.
30. Yu Q, Tao Z, Wu YX. Experimental behaviour of high performance concrete-filled steel tubular columns. *Thin-Walled Structures*. 2008;46(4): 362-370.
31. Han LH, Yao GH. Experimental behaviour of thin-walled hollow structural steel (HSS) columns filled with self-consolidating concrete (SCC). *Thin-Walled Structures*. 2004;42(9): 1357-1377.
32. Han LH, Liao FY, Tao Z, Hong Z. Performance of concrete filled steel tube reinforced concrete columns subjected to cyclic bending. *Journal of Constructional Steel Research*. 2009;65(8): 1607-1616.
33. Campian C, Pacurar V, Petran I, Bale R. Monotonic and cyclic behaviour of fully encased composite columns. In *Steel-A New and Traditional Material for Building: Proceedings of the International Conference in Metal Structures 2006, 20-22 September 2006, Poiana Brasov, Romania*. CRC Press; 2006.
34. Karimi K, El-Dakhkhni WW, Tait MJ. Behavior of slender steel-concrete composite columns wrapped with FRP jackets. *Journal of Performance of Constructed Facilities*. 2011;26(5): 590-599.
35. Lachance L. Ultimate strength of biaxially loaded composite sections. *Journal of the Structural Division*. 1982;108(10): 2313-2329.
36. Morino S, Matsui C, Watanabe H. Strength of biaxially loaded SRC columns. In *Composite and mixed construction*. ASCE; 1984. p. 185-194.
37. Munoz PR, Hsu CTT. Biaxially loaded concrete-encased composite columns: design equation. *Journal of structural engineering*. 1997;123(12): 1576-1585.
38. Ricles JM, Paboojian SD. Seismic performance of steel-encased composite columns. *Journal of Structural Engineering*. 1994;120(8): 2474-2494.
39. Chen CC, Lin NJ. Analytical model for predicting axial capacity and behavior of concrete encased steel composite stub columns. *Journal of Constructional Steel Research*. 2006;62(5): 424-433.
40. Campian C, Nagy Z, Pop M. Behavior of Fully Encased Steel-concrete Composite Columns Subjected to Monotonic and Cyclic Loading. *Procedia Engineering*. 2015;117: 444-456.
41. Dundar C, Tokgoz S, Tanrikulu AK, Baran T. Behaviour of reinforced and concrete-encased composite columns subjected to biaxial bending and axial load. *Building and environment*. 2008;43(6): 1109-1120.
42. Yu T, Lin G, Zhang SS. Compressive behavior of FRP-confined concrete-encased steel columns. *Composite Structures*. 2016;154: 493-506.
43. Chen CC, Li JM, Weng CC. Experimental behaviour and strength of concrete-encased composite beam-columns with T-shaped steel section under cyclic loading. *Journal of Constructional Steel Research*. 2005;61(7): 863-881.
44. Elnashai AS, Elghazouli AY, Takanashi K, Dowling PJ. Experimental behaviour of partially encased composite beam-columns under cyclic and dynamic loads. *Institution of Civil Engineers Proceedings pt.* 1991;2: 259-72.
45. Lelkes A, Gramblička Š. Theoretical and Experimental Studies on Composite Steel-Concrete Columns. *Procedia Engineering*. 2013;65: 405-410.
46. Papavasileiou GS. *Simulation of steel and concrete composite columns with equivalent pure-steel sections*. Democritus University of Thrace, Greece; 2007. [in Greek]
47. Marinopoulou AA, Balopoulos VD, Kalfas CN. Simulation of partially encased composite steel-concrete columns with steel columns. *Journal of Constructional Steel Research*. 2007;63(8): 1058-1065.
48. CEN. *EN-1994-1-1: Eurocode 4: Design of composite steel and concrete structures - Part 1-1: General rules and rules for buildings*. European Committee for Standardization; 2004.
49. CEN. *EN-1993-1-1: Eurocode 3: Design of steel structures - Part 1-1: General rules and rules for buildings*. European Committee for Standardization; 2005.
50. CEN. *EN-1992-1-1: Eurocode 2: Design of concrete structures - Part 1-1: General rules and rules for buildings*. European Committee for Standardization; 2004.
51. Burg RG, Ost BW. *Engineering Properties of Commercially Available High-Strength Concretes (Including Three-Year Data)*. Report No. RD104. 02T, 1994.

52. Chan, CM. Optimal lateral stiffness design of tall buildings of mixed steel and concrete construction. *The Structural Design of Tall Buildings*. 2001;10(3): 155-177.
53. Papavasileiou GS, Charmpis DC. Seismic design optimization of multi-storey steel-concrete composite buildings. *Computers & Structures*. 2016;170: 49-61. doi:10.1016/j.compstruc.2016.03.010
54. Cheng L, Chan CM. Optimal lateral stiffness design of composite steel and concrete tall frameworks. *Engineering structures*. 2009;31(2): 523-533.
55. Lagaros ND, Magoula E. Life-cycle cost assessment of mid-rise and high-rise steel and steel-reinforced concrete composite minimum cost building designs. *The Structural Design of Tall and Special Buildings*. 2013;22(12): 954-974.
56. Luo Y, Wang MY, Zhou M, Deng Z. Optimal topology design of steel-concrete composite structures under stiffness and strength constraints. *Computers & Structures*. 2012;112: 433-444.